NASA TECHNICAL MEMORANDUM

NASA TM X-53002

N64-15623 mfo

CODE-1

69p.

NASA TM X-53002

PERFORMANCE ANALYSIS OF CHEMICAL STAGES IN THE 300 TO 400 SECOND SPECIFIC IMPULSE RANGE FOR INTERPLANETARY MISSIONS

by WALTER H. STAFFORD and CARMEN R. CATALFAMO
~~Propulsion and Vehicle Engineering Laboratory~~
NASA.

George C. Marshall Space Flight Center, Huntsville, Alabama

Washington, NASA, 5 Feb. 1964 69p mfo

NATIONAL AERONAUTICS AND SPACE ADMINISTRATION · WASHINGTON, D. C. · FEBRUARY 5, 1964

GEORGE C. MARSHALL SPACE FLIGHT CENTER

NASA TM X-53,002

PERFORMANCE ANALYSIS OF CHEMICAL STAGES IN THE 300 TO 400 SECOND SPECIFIC IMPULSE RANGE FOR INTERPLANETARY MISSIONS

By

Walter H. Stafford and Carmen R. Catalfamo

ABSTRACT

15623

The purpose of this report is to present a procedure by which trajectory parameters can be determined for escaping from, and braking into, an orbit about the earth utilizing a single vehicle stage in the low specific impulse range.

The data are presented in two sections: Section A is for escape from an orbit about the earth and Section B is for braking into an orbit about the earth.

The effect of thrust-to-weight ratios and specific impulses on trajectory parameters was investigated for hyperbolic velocities. For the escape trajectories, the thrust vector was applied tangential to the flight path and in the direction of the velocity vector. For the braking trajectories, the thrust vector was directed against the velocity vector. Specific impulses of 300 to 400 seconds and earth thrust-to-weight ratios of 0.2 to 1.0 were used.

The approach used for the escape trajectories was to determine the trajectory parameters at burnout, convert the characteristic velocity to a hyperbolic excess velocity and then present the data graphically. The approach used for the braking trajectories was to determine the arrival velocity for a given transfer trajectory and initiate burning such that circular orbit conditions are attained at burnout. The characteristic velocity is converted to a hyperbolic excess velocity and presented graphically.

Author

GEORGE C. MARSHALL SPACE FLIGHT CENTER

NASA TM X-53,002

PERFORMANCE ANALYSIS OF CHEMICAL STAGES IN THE 300 TO 400 SECOND SPECIFIC IMPULSE RANGE FOR INTERPLANETARY MISSIONS

By

Walter H. Stafford and Carmen R. Catalfamo

MISSION ANALYSIS GROUP
ADVANCED STUDIES OFFICE
PROPULSION AND VEHICLE ENGINEERING LABORATORY

TABLE OF CONTENTS

LIST OF ILLUSTRATIONS

LIST OF ILLUSTRATIONS (Continued)

LIST OF ILLUSTRATIONS (Continued)

LIST OF ILLUSTRATIONS (Continued)

LIST OF ILLUSTRATIONS (Continued)

LIST OF ILLUSTRATIONS (Concluded)

DEFINITION OF SYMBOLS

Symbol	Definition
F	Thrust, N
F/W_o	Initial thrust-to-weight ratio (based on weight at earth sea level)
f	Stage mass fraction, (W_P/W_A)
g	Gravitational acceleration, m/sec^2
H	Energy
h	Altitude, km
Δh	Altitude change, $(h - h_o)$, km
I_{sp}	Specific impulse, sec
m	Mass, kg
r	Radius, km
R	Planet radius, km
r_o	$(h_o + R)$, km
t_B	Burning time, sec
V	Velocity
V^*	Comparative velocity
V_1	Stage characteristic velocity
V_∞	Hyperbolic excess velocity
W_A	Stage weight, $(W_o - W_L)$, N
W_L	Payload weight, N

DEFINTION OF SYMBOLS (Continued)

Symbol	Definition
W_o	Gross weight, N
W_P	Propellant weight, N
X	Range, km
α	Angle of attack (angle between velocity vector and thrust vector), deg
ζ	Propellant mass fraction, (W_P/W_o)
ϑ	Flight path angle from vertical, deg
μ	Gravitational constant
ψ	Central angle, deg
Subscripts	
C	Burnout
esc	Escape
ex	Exhaust
f	Final
id	Ideal
K	Circular
o	Initial
P	Propellant

DEFINITION OF SYMBOLS (Concluded)

Symbol	Definition
Abbreviations	
kg	Kilogram
km	Kilometer
m	Meter
sec	Second
N	Newton

GEORGE C. MARSHALL SPACE FLIGHT CENTER

NASA TM X-53,002

PERFORMANCE ANALYSIS OF CHEMICAL STAGES IN THE 300 TO 400 SECOND SPECIFIC IMPULSE RANGE FOR INTERPLANETARY MISSIONS

By

Walter H. Stafford and Carmen R. Catalfamo

SUMMARY

The effect of thrust-to-weight ratios and specific impulses on trajectory parameters has been investigated for hyperbolic escape from, and braking into, an orbit about earth. For the escape trajectories, the thrust vector was applied tangential to the flight path and in the direction of the velocity vector. For the braking-in trajectories, the thrust vector was directed against the velocity vector. Thrust-to-weight ratios of 0.2 to 1.0 and specific impulses of 300 to 400 seconds were used.

The results of the study are presented graphically.

SECTION I. INTRODUCTION

A study of the trajectory requirements is of fundamental importance in planning interplanetary round-trip missions. Preliminary analysis of the mission requires a rapid method of sufficient accuracy for determining the trajectory parameters. The sizing of boost vehicles is dependent, to a large extent, on the velocity requirements of the particular trajectory chosen.

The purpose of this study is to present a method for determining the trajectory parameters and vehicle mass characteristics for a specific mission, when the hyperbolic excess velocity is known.

The approach used for escape from orbit was to determine the trajectory parameters at burnout, convert the characteristic velocity to a hyperbolic excess velocity, and then present the data graphically. The approach used for braking into orbit was to determine the arrival velocity for a given transfer trajectory and initiate burning such that circular orbit conditions are attained at burnout. The equations of motion were integrated on a digital computer, using a Runge-Kutta numerical integration procedure.

SECTION II. ASSUMPTIONS

The following is a summary of the basic assumptions used in this study:

1. For escape -- Acceleration of a single stage from a reference orbit about earth, using a constant thrust directed along the velocity vector.

2. For braking -- Deceleration of a single stage from an interplanetary transfer trajectory to a reference orbit about earth, using a constant thrust directed against the velocity vector.

3. Reference orbit about the earth was circular with a radius of 6556 km and a velocity of 7798 m/sec.

4. Constant specific impulse values from 300 to 400 seconds.

5. The thrust-to-weight ratios used were varied parametrically from 0.2 to 1.0.

6. Mean spherical earth:

$$\mu = 398606.6 \text{ km}^3/\text{sec}^2$$

$$R = 6371.27 \text{ km}$$

SECTION III. ANALYSIS

For interplanetary flight, the ideal[1] total energy that must be imparted to the spacecraft is the ideal energy required to escape the

---

(1) The term "ideal" refers to an instantaneous change of energy.

gravitational field of the planet, plus the energy required to change its path about the Sun. The ideal energy required to escape the gravitational attraction of a planet can be determined from two-body mechanics to be $H_{esc} = \mu/r$ and the energy needed to alter the flight path about the Sun, H_∞, is determined by the characteristics of the interplanetary trajectory.

For determining the vehicle size necessary to inject the spacecraft into the interplanetary trajectory, it is convenient to express the ideal total energy, $H = H_{esc} + H_\infty$, in terms of a burnout velocity. This produces equations of the following forms:

$$V_C = \sqrt{H_{esc} + H_\infty} \tag{1}$$

or

$$V_C = \sqrt{(V_{esc})^2 + (V_\infty)^2} \tag{2}$$

When considering finite vehicle systems there is an additional energy requirement, H_{loss}, which results from expending the propellants at different energy levels. Therefore, the total velocity increment for the injecting stage is now

$$V_1 = V_C - V_o + V_{loss} \tag{3}$$

where V_o is the initial velocity. The vehicle mass characteristics can be determined from the equation

$$\frac{W_o}{W_C} = e^{\frac{V_1}{V_{ex}}} \tag{4}$$

To accomplish this study, the two-degree-of-freedom equations of motion were numerically integrated.

Referring to the sketches, "a" for escaping from and "b" for braking into, computations were made for a point mass moving in a plane using the following equations of motion:

$$\dot{V} = \frac{F \cos \alpha}{m} - \frac{\mu}{r^2} \cos \vartheta \tag{5}$$

$$V \dot{\vartheta} = \frac{F \sin \alpha}{m} + \left(\frac{\mu}{r^2} - \frac{V^2}{r} \right) \sin \vartheta \tag{6}$$

$$\dot{r} = V \cos \vartheta \tag{7}$$

$$\dot{\psi} = \frac{V \sin \vartheta}{r} \tag{8}$$

where

$$m = m_o + \int \dot{m}\, dt \tag{9}$$

and

$$\dot{m} = - \frac{F}{V_{ex}} \tag{10}$$

The velocity and flight path angle may be obtained by integrating the equations of motion

$$V = V_o + \int \dot{V}\, dt \tag{11}$$

$$\vartheta = \vartheta_o + \int \dot{\vartheta}\, dt \tag{12}$$

The range and pericenter altitude can then be calculated by the relations

$$X = X_o + \int \frac{R}{r} V \sin \vartheta\, dt \tag{13}$$

$$h = h_o + \int \dot{r}\, dt \tag{14}$$

The central angle is

$$\psi = \psi_o + \int \frac{\dot{X}}{R}\, dt \tag{15}$$

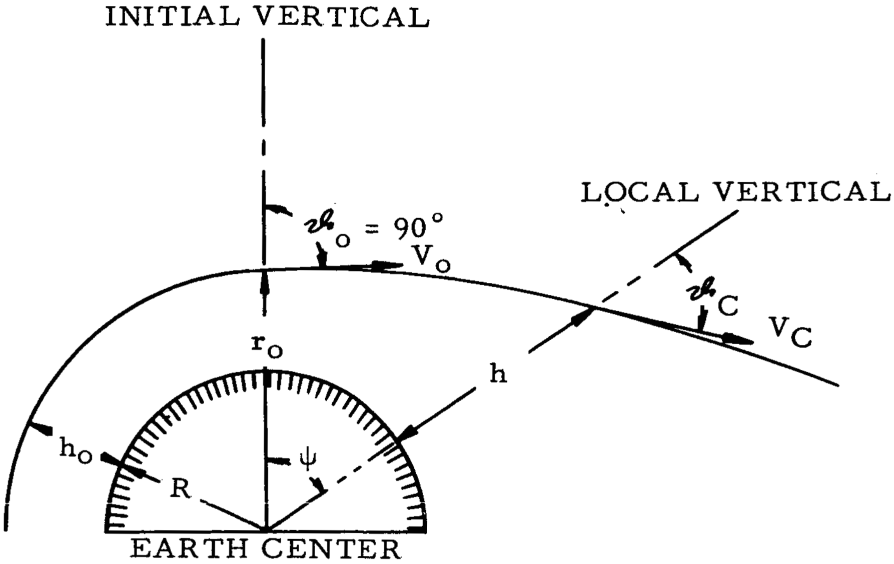

SKETCH a. ESCAPE FROM ORBIT

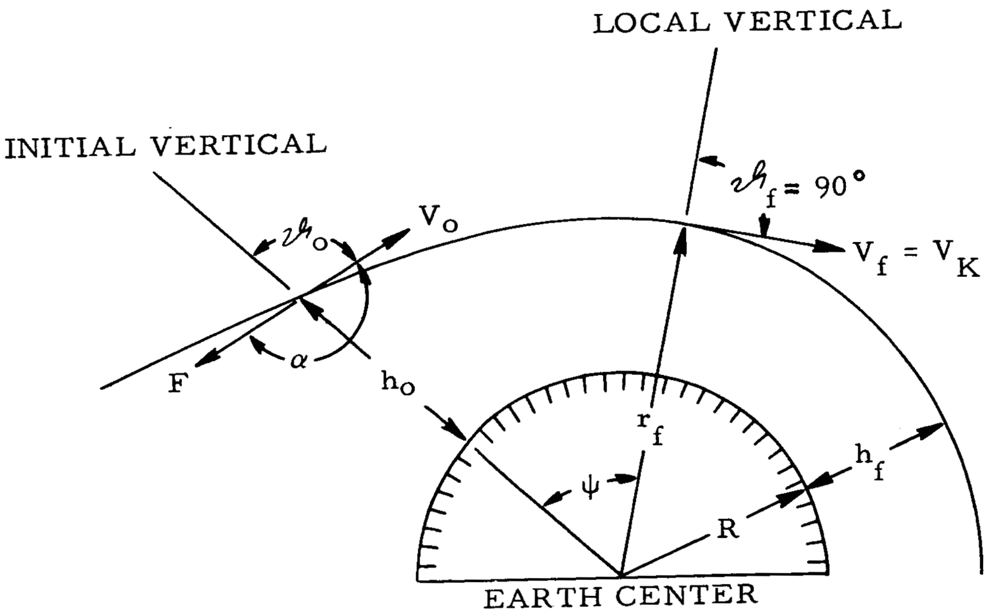

SKETCH b. BRAKE TO ORBIT

The initial weight of the stage is

$$W_o = W_C + W_P \tag{16}$$

The velocity expended by the stage is the characteristic velocity, or

$$V_1 = V_{ex} \ln \left(\frac{1}{1 - \zeta} \right) \tag{17}$$

Then the velocity losses are the difference between the characteristic velocity and the change in comparative velocity, or

$$V_{loss} = V_1 - \Delta V^* \tag{18}$$

where the comparative velocity is

$$V^* = \sqrt{V^2 + 2\mu \left(\frac{1}{R} - \frac{1}{r} \right)} \tag{19}$$

For ascent from $r = r_o$ to $r = r_f$, the change in comparative velocity is

$$\Delta V^* = \sqrt{V_f^2 + 2\mu \left(\frac{1}{r_o} - \frac{1}{r_f} \right)} - V_o \tag{20}$$

and the velocity loss due to gravity is

$$V_{loss} = V_{ex} \ln \left(\frac{1}{1 - \zeta} \right) - \left[\sqrt{V_f^2 + 2\mu \left(\frac{1}{r_o} - \frac{1}{r_f} \right)} - V_o \right] \tag{21}$$

For descent from $r = r_o$ to $r = r_f$, the change in comparative velocity is

$$\Delta V^* = \sqrt{V_o^2 + 2\mu \left(\frac{1}{r_f} - \frac{1}{r_o} \right)} - V_f \tag{22}$$

and the velocity loss due to gravity is

$$V_{loss} = V_{ex} \ln \left(\frac{1}{1 - \zeta} \right) - \left[\sqrt{V_o^2 + 2\mu \left(\frac{1}{r_f} - \frac{1}{r_o} \right)} - V_f \right] \tag{23}$$

SECTION IV. DISCUSSION OF RESULTS

The results of this investigation are presented grahically in Figures 1 through 11 for each of the two areas considered.[2] The stage characteristic velocity, V_1, is plotted versus hyperbolic excess velocity, with thrust-to-weight ratios as a parameter, in Figures 1 through 5.

Figures 6 and 7 show the velocity losses, V_{loss}, due to gravity for specific impulse values of 300 seconds and 400 seconds, respectively. The flight path angle at burnout for departure trajectories and at initiation of burning for braking trajectories, is shown versus hyperbolic excess velocity in Figure 8.

Figure 9 gives the change in altitude. This change is the difference between the altitude of the reference orbit about the planet and the altitude at burnout for the departure trajectories, and the difference between the altitude of the reference orbit and the altitude at initiation of burning for braking trajectories. The change in other trajectory parameters is shown in Figures 10 and 11.

The vehicle mass characteristics can be determined from Figures 12 and 13 in the Section entitled "Brake to Earth Orbit."

SECTION V. CONCLUSIONS

From these parametric analyses, sufficient data are provided to enable the designer to make a preliminary design of a stage that will accomplish any one of the mission areas studied when that particular mission's requirements are defined.

---

(2)Figure references apply to each of the two areas considered.

SECTION VI. GRAPHIC PRESENTATION

DEPARTURE FROM EARTH ORBIT

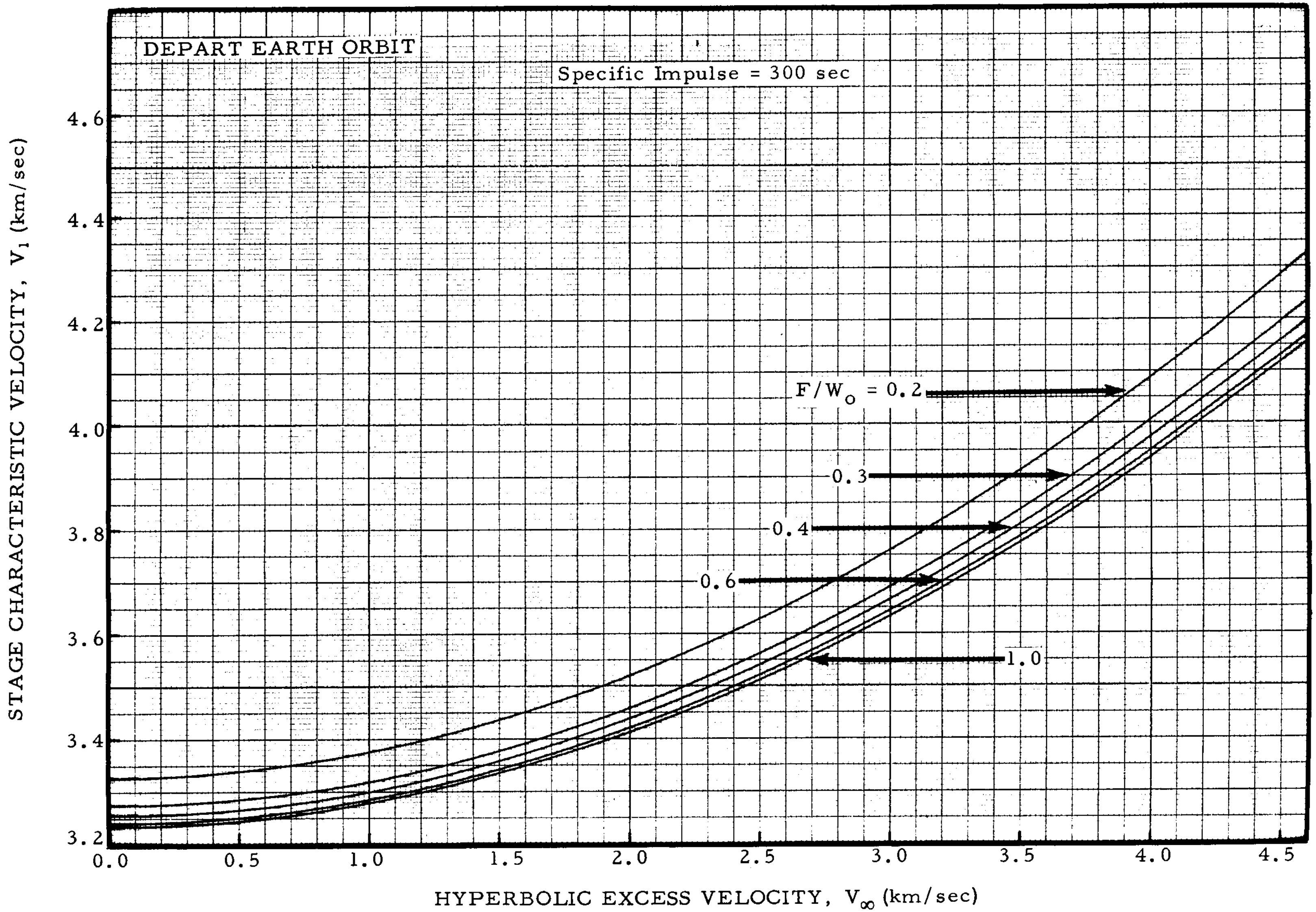

FIGURE 1a. CHARACTERISTIC VELOCITY, V_1 (km/sec), VERSUS HYPERBOLIC EXCESS VELOCITY, V_∞ (km/sec), WITH THRUST-TO-WEIGHT RATIO AS A PARAMETER FOR A CONSTANT SPECIFIC IMPULSE OF 300 SECONDS

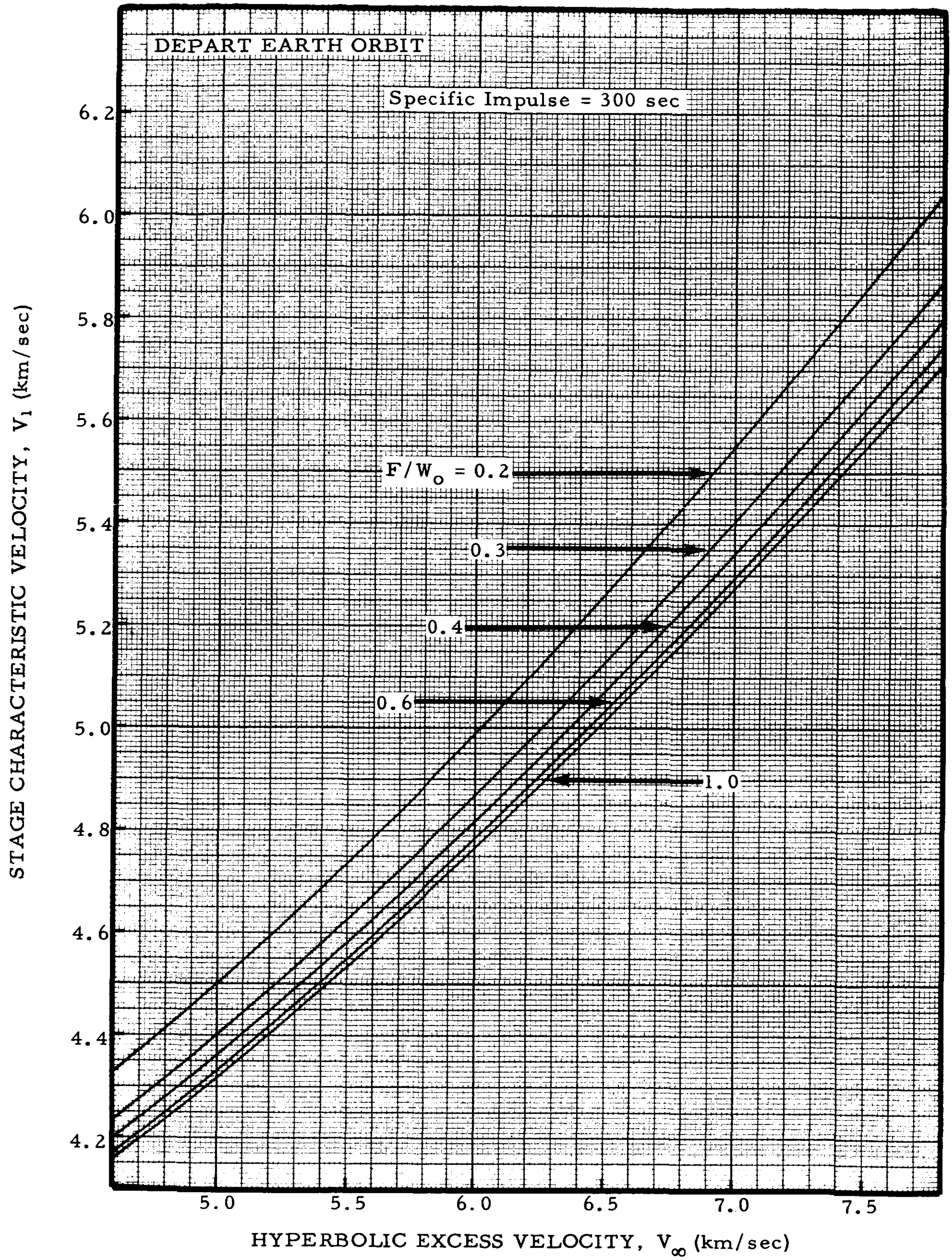

FIGURE 1b. CHARACTERISTIC VELOCITY, V_1 (km/sec), VERSUS HYPERBOLIC EXCESS VELOCITY, V_∞ (km/sec), WITH THRUST-TO-WEIGHT RATIO AS A PARAMETER FOR A CONSTANT SPECIFIC IMPULSE OF 300 SECONDS

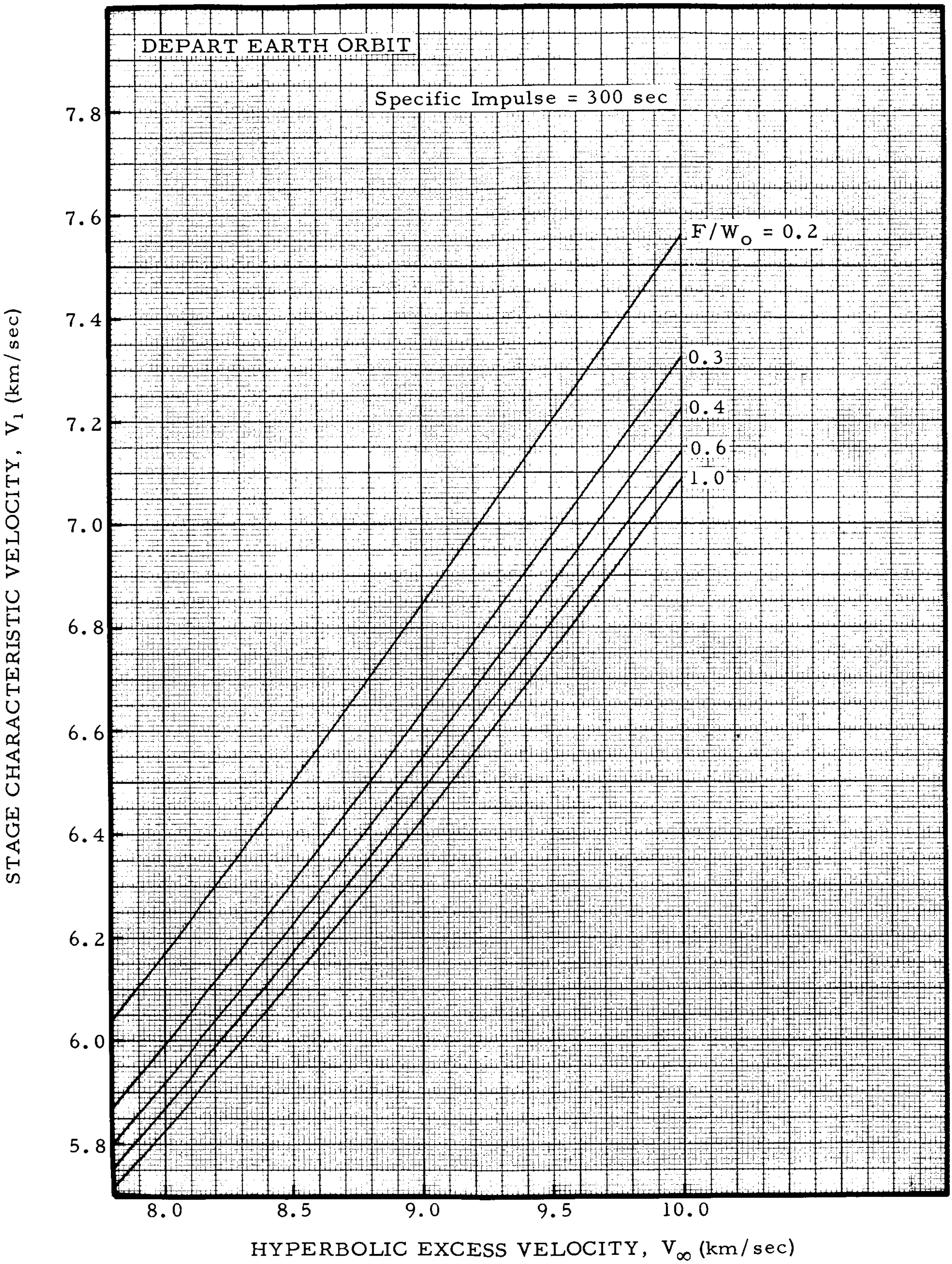

FIGURE 1c. CHARACTERISTIC VELOCITY, V_1 (km/sec), VERSUS HYPERBOLIC EXCESS VELOCITY, V_∞ (km/sec), WITH THRUST-TO-WEIGHT RATIO AS A PARAMETER FOR A CONSTANT SPECIFIC IMPULSE OF 300 SECONDS

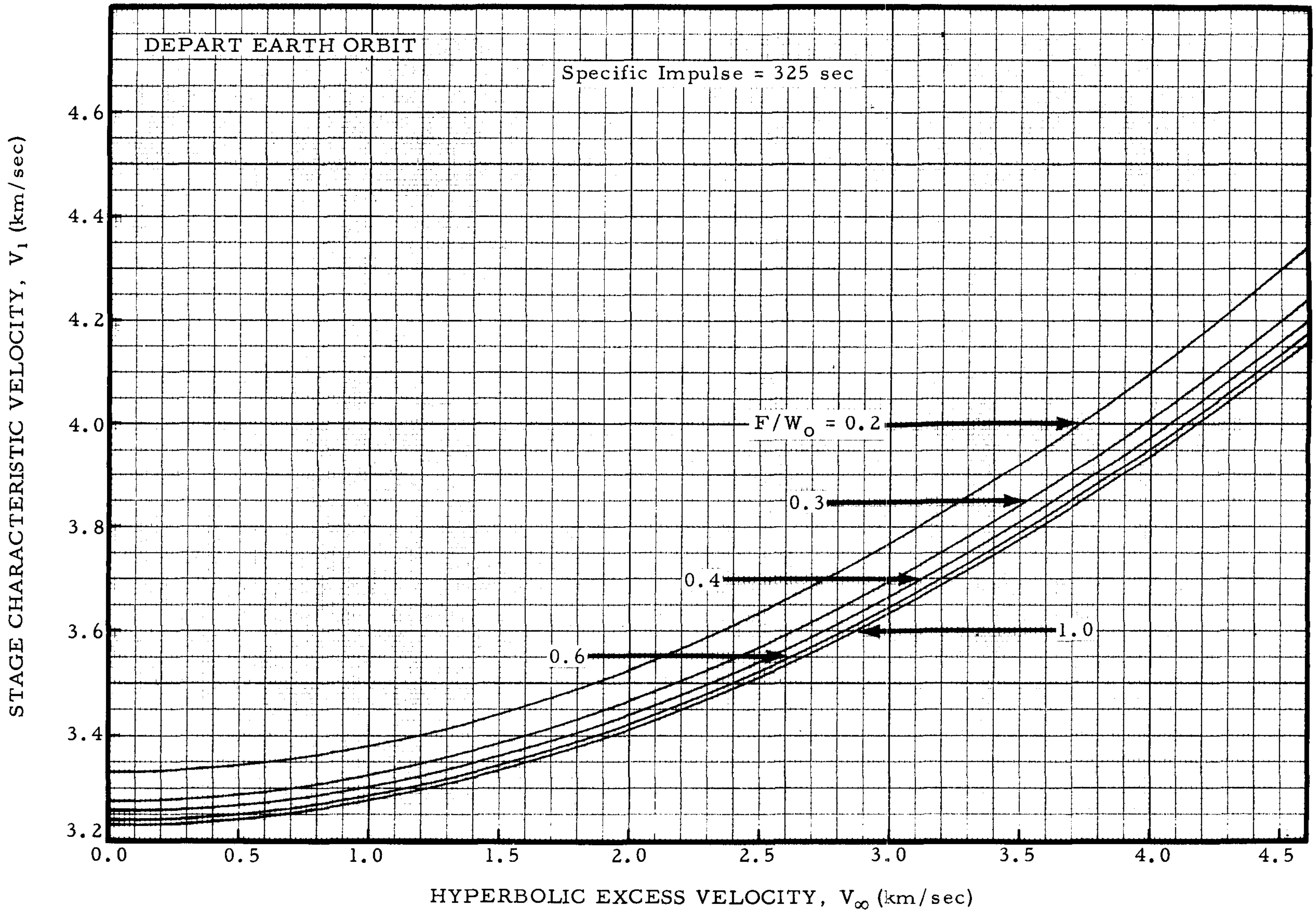

FIGURE 2a. CHARACTERISTIC VELOCITY, V_1 (km/sec), VERSUS HYPERBOLIC EXCESS VELOCITY, V_∞ (km/sec), WITH THRUST-TO-WEIGHT RATIO AS A PARAMETER FOR A CONSTANT SPECIFIC IMPULSE OF 325 SECONDS

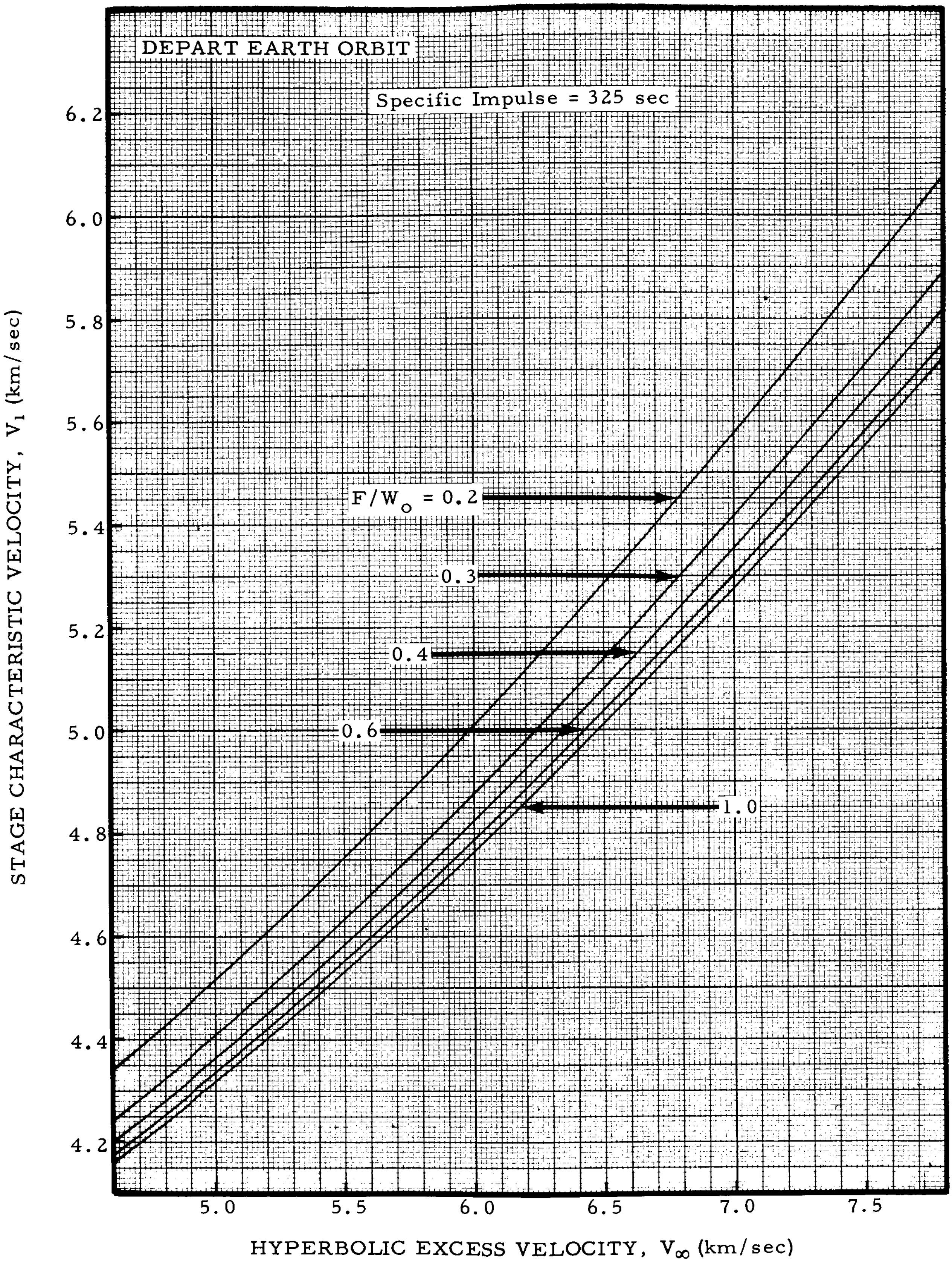

FIGURE 2b. CHARACTERISTIC VELOCITY, V_1 (km/sec), VERSUS HYPERBOLIC EXCESS VELOCITY, V_∞ (km/sec), WITH THRUST-TO-WEIGHT RATIO AS A PARAMETER FOR A CONSTANT SPECIFIC IMPULSE OF 325 SECONDS

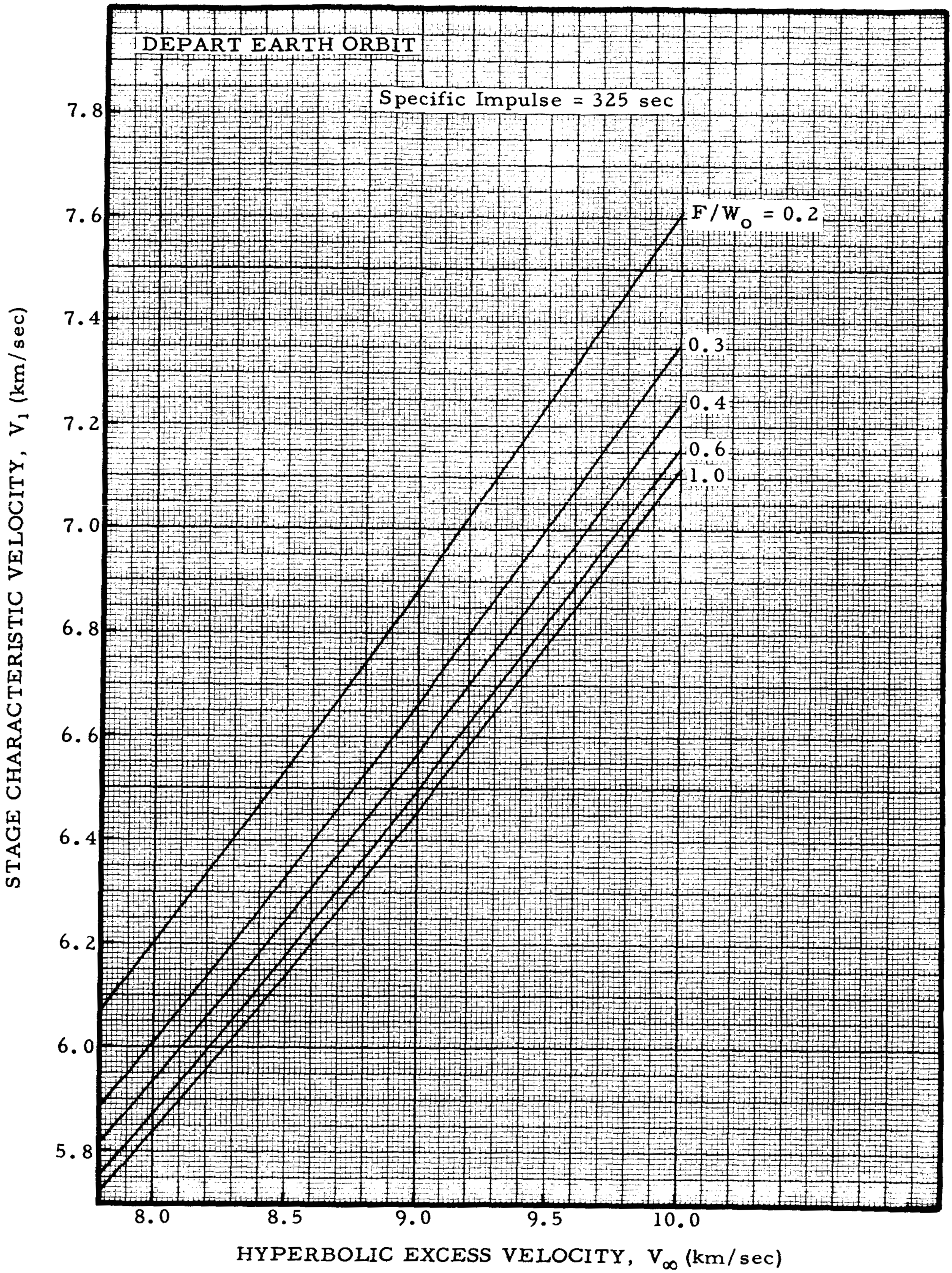

FIGURE 2c. CHARACTERISTIC VELOCITY, V_1 (km/sec), VERSUS HYPERBOLIC EXCESS VELOCITY, V_∞ (km/sec), WITH THRUST-TO-WEIGHT RATIO AS A PARAMETER FOR A CONSTANT SPECIFIC IMPULSE OF 325 SECONDS

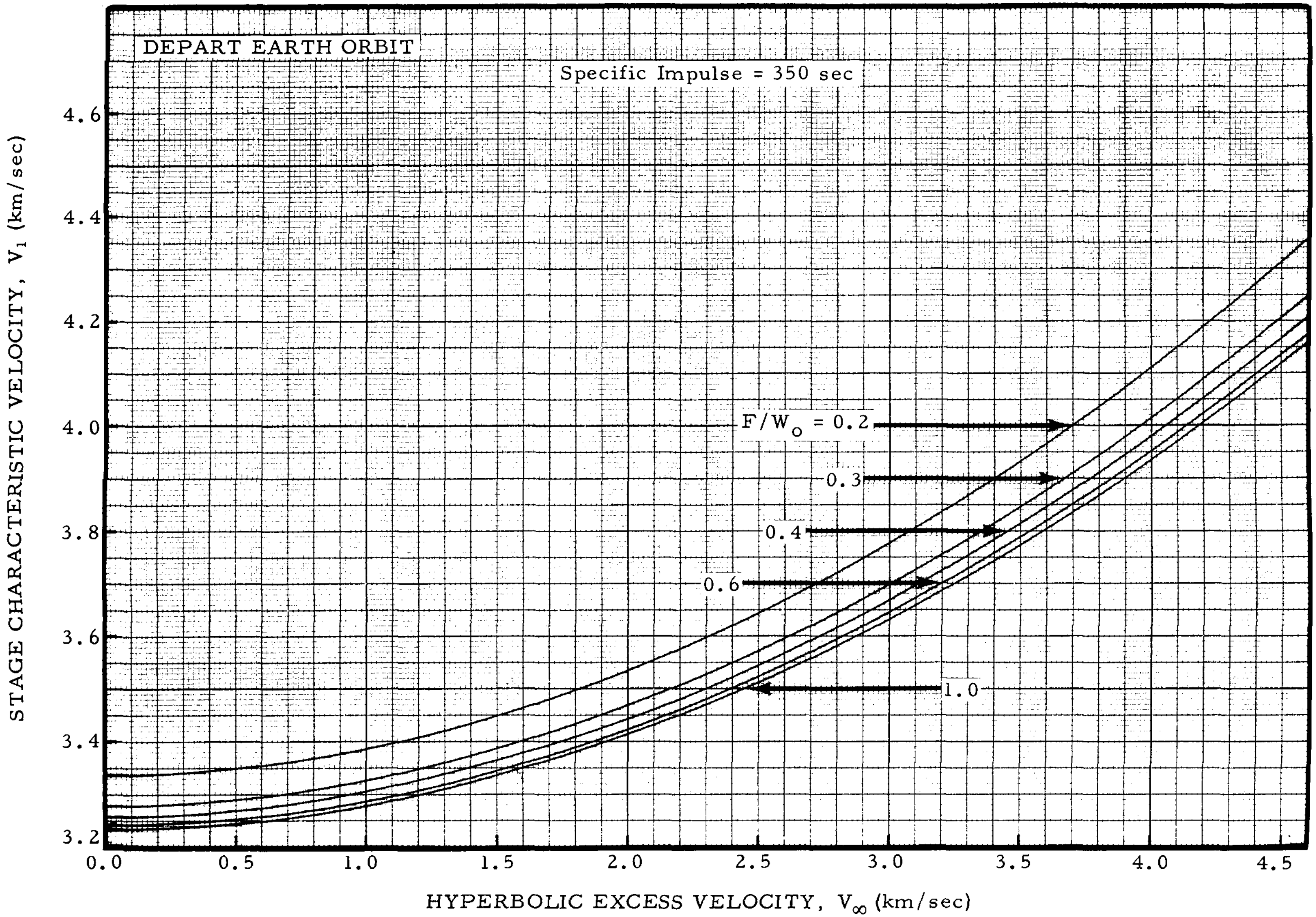

FIGURE 3a. CHARACTERISTIC VELOCITY, V_1 (km/sec), VERSUS HYPERBOLIC EXCESS VELOCITY, V_∞ (km/sec), WITH THRUST-TO-WEIGHT RATIO AS A PARAMETER FOR A CONSTANT SPECIFIC IMPULSE OF 350 SECONDS

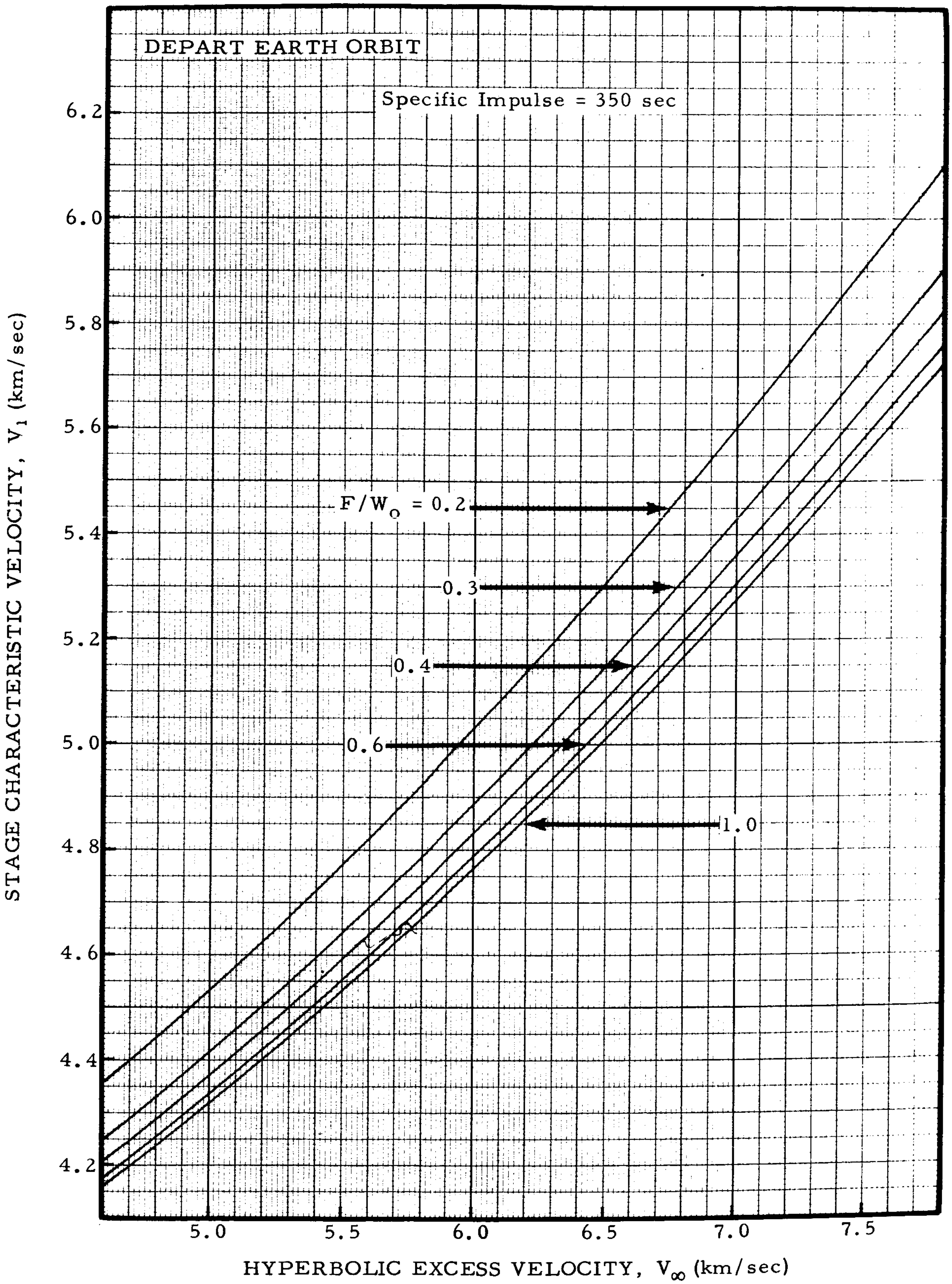

FIGURE 3b. CHARACTERISTIC VELOCITY, V_1 (km/sec), VERSUS HYPERBOLIC EXCESS VELOCITY, V_∞ (km/sec), WITH THRUST-TO-WEIGHT RATIO AS A PARAMETER FOR A CONSTANT SPECIFIC IMPULSE OF 350 SECONDS

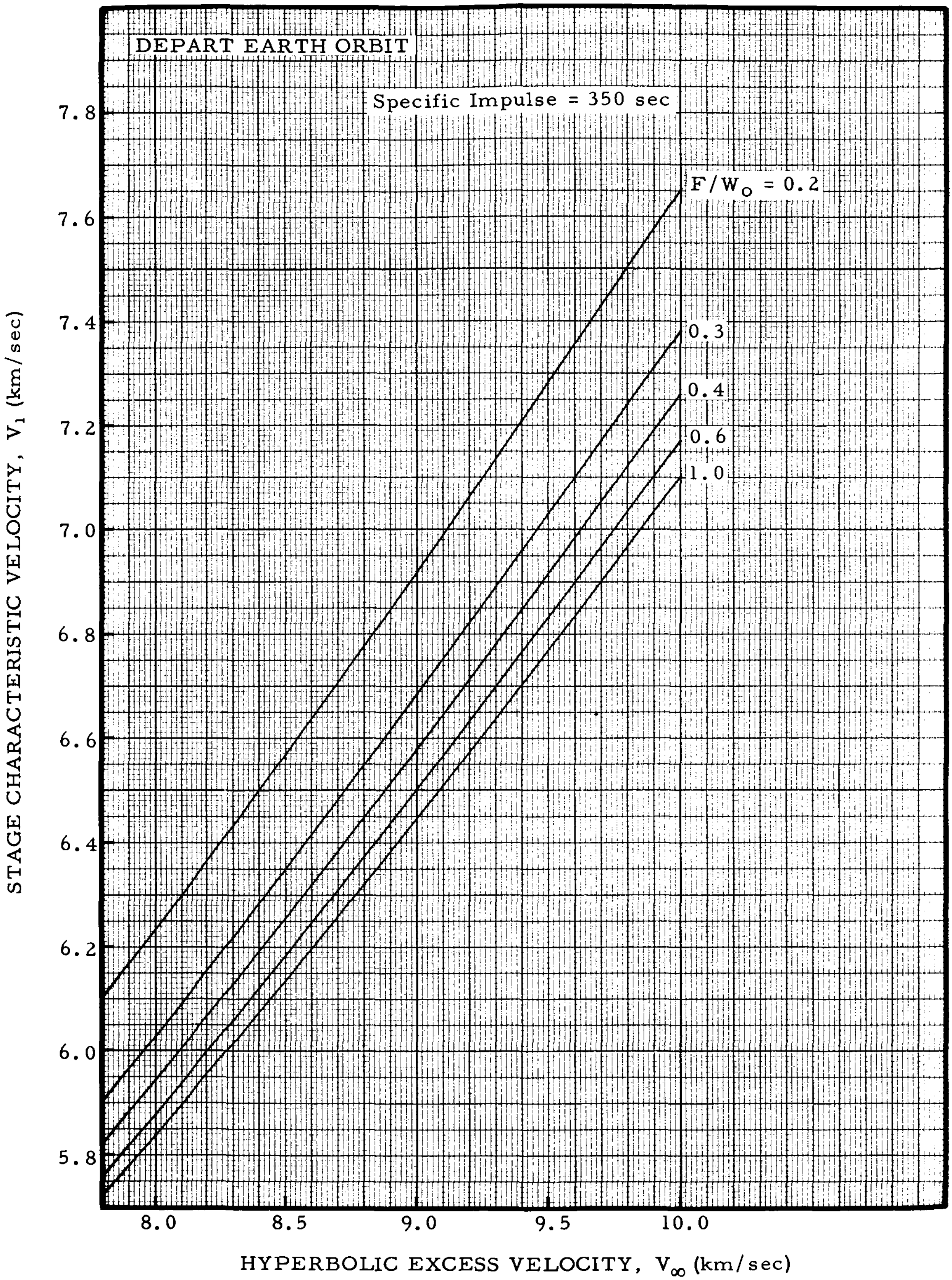

FIGURE 3c. CHARACTERISTIC VELOCITY, V_1 (km/sec), VERSUS HYPERBOLIC EXCESS VELOCITY, V_∞ (km/sec), WITH THRUST-TO-WEIGHT RATIO AS A PARAMETER FOR A CONSTANT SPECIFIC IMPULSE OF 350 SECONDS

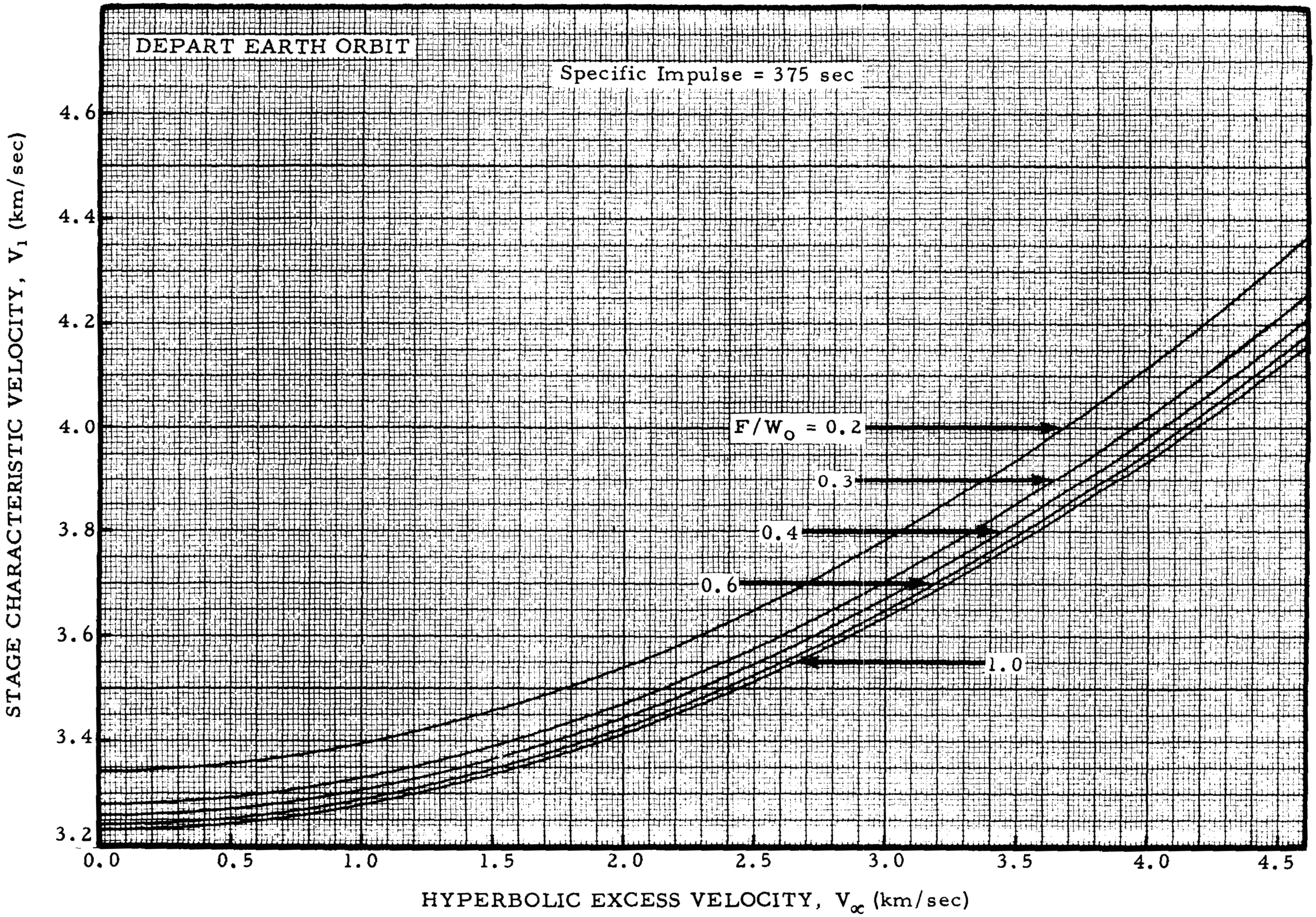

FIGURE 4a. CHARACTERISTIC VELOCITY, V_1 (km/sec), VERSUS HYPERBOLIC EXCESS VELOCITY, V_∞ (km/sec), WITH THRUST-TO-WEIGHT RATIO AS A PARAMETER FOR A CONSTANT SPECIFIC IMPULSE OF 375 SECONDS

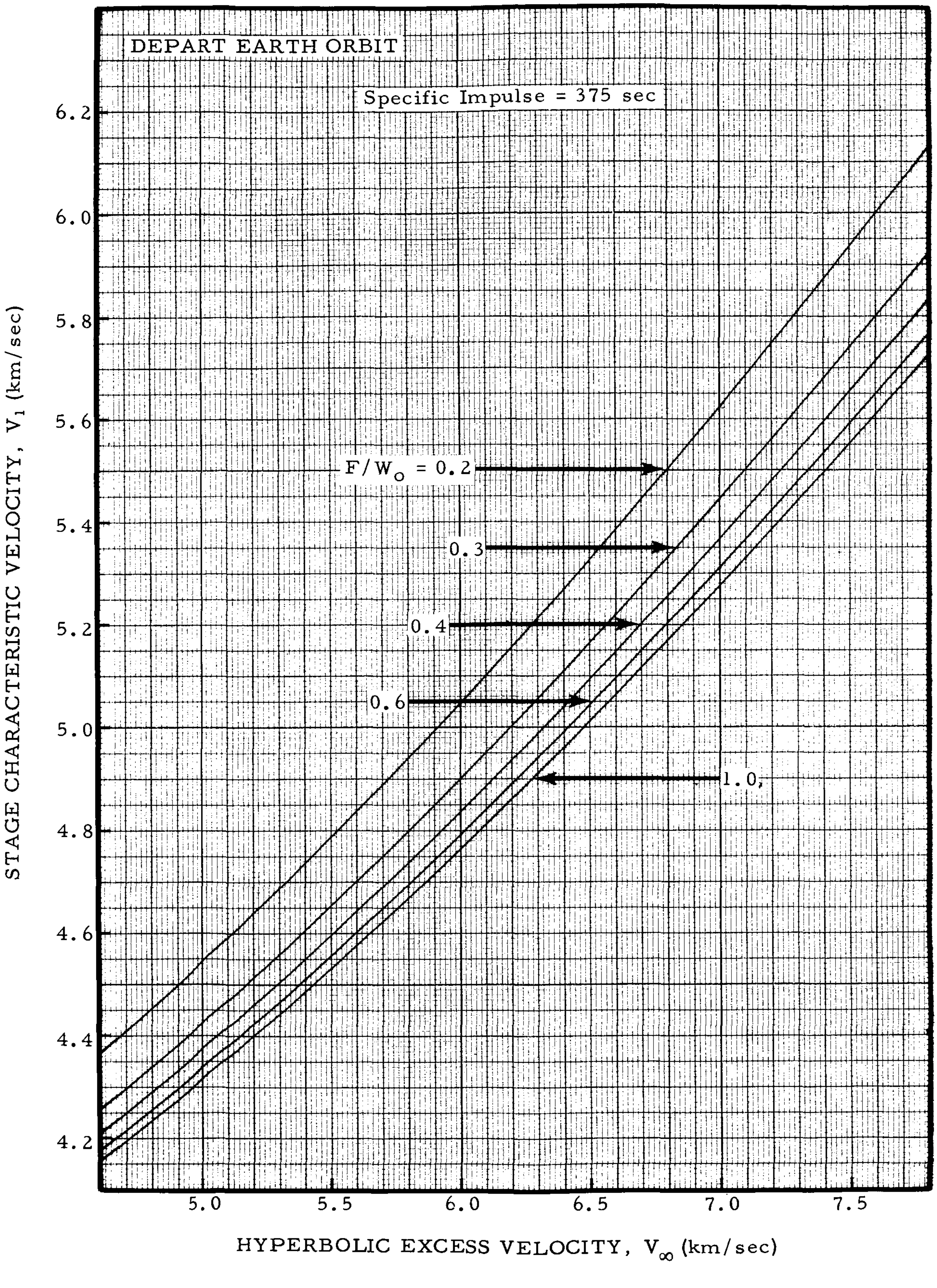

FIGURE 4b. CHARACTERISTIC VELOCITY, V_1 (km/sec), VERSUS HYPERBOLIC EXCESS VELOCITY, V_∞ (km/sec), WITH THRUST-TO-WEIGHT RATIO AS A PARAMETER FOR A CONSTANT SPECIFIC IMPULSE OF 375 SECONDS

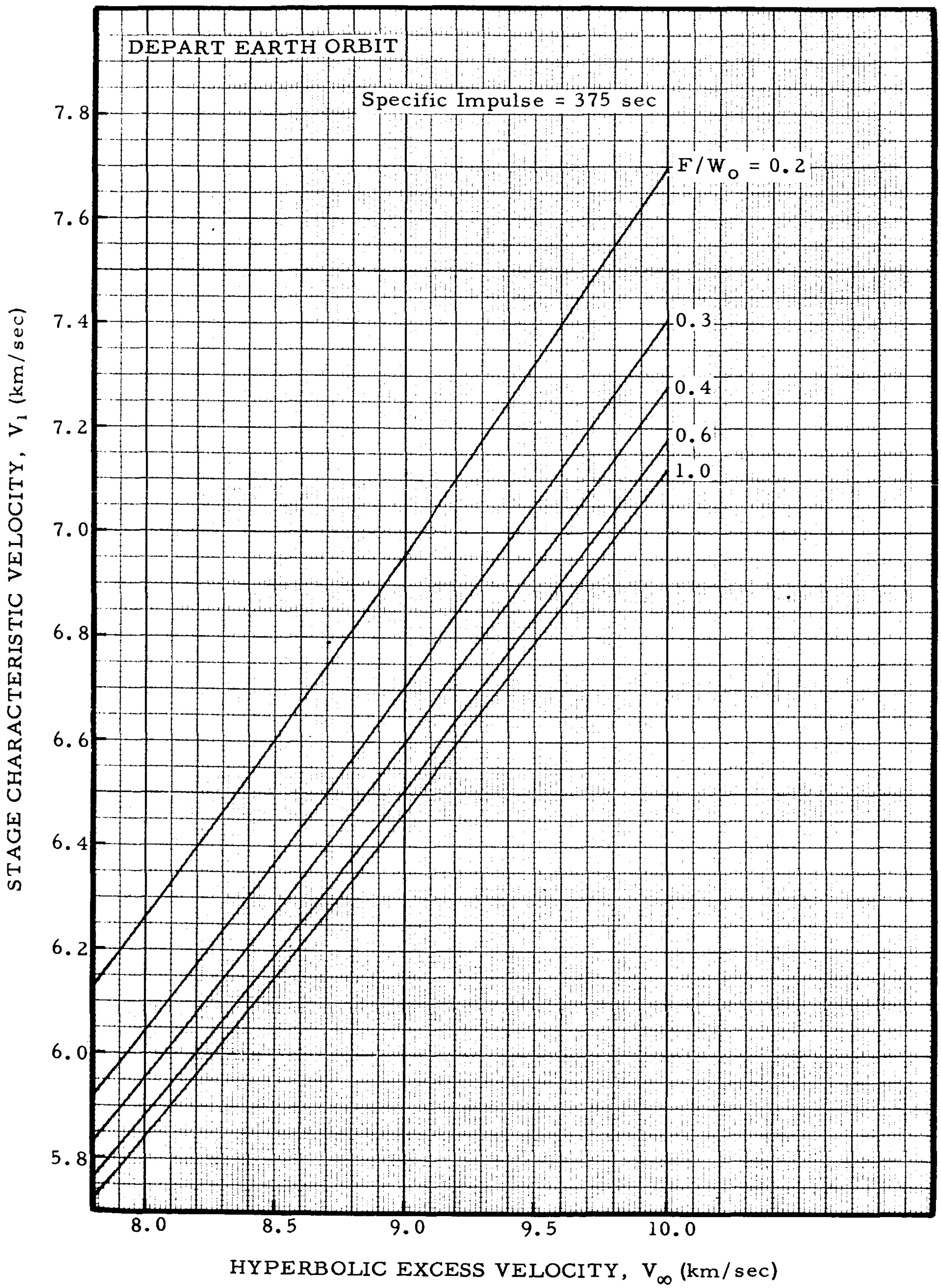

FIGURE 4c. CHARACTERISTIC VELOCITY, V_1 (km/sec), VERSUS HYPERBOLIC EXCESS VELOCITY, V_∞ (km/sec), WITH THRUST-TO-WEIGHT RATIO AS A PARAMETER FOR A CONSTANT SPECIFIC IMPULSE OF 375 SECONDS

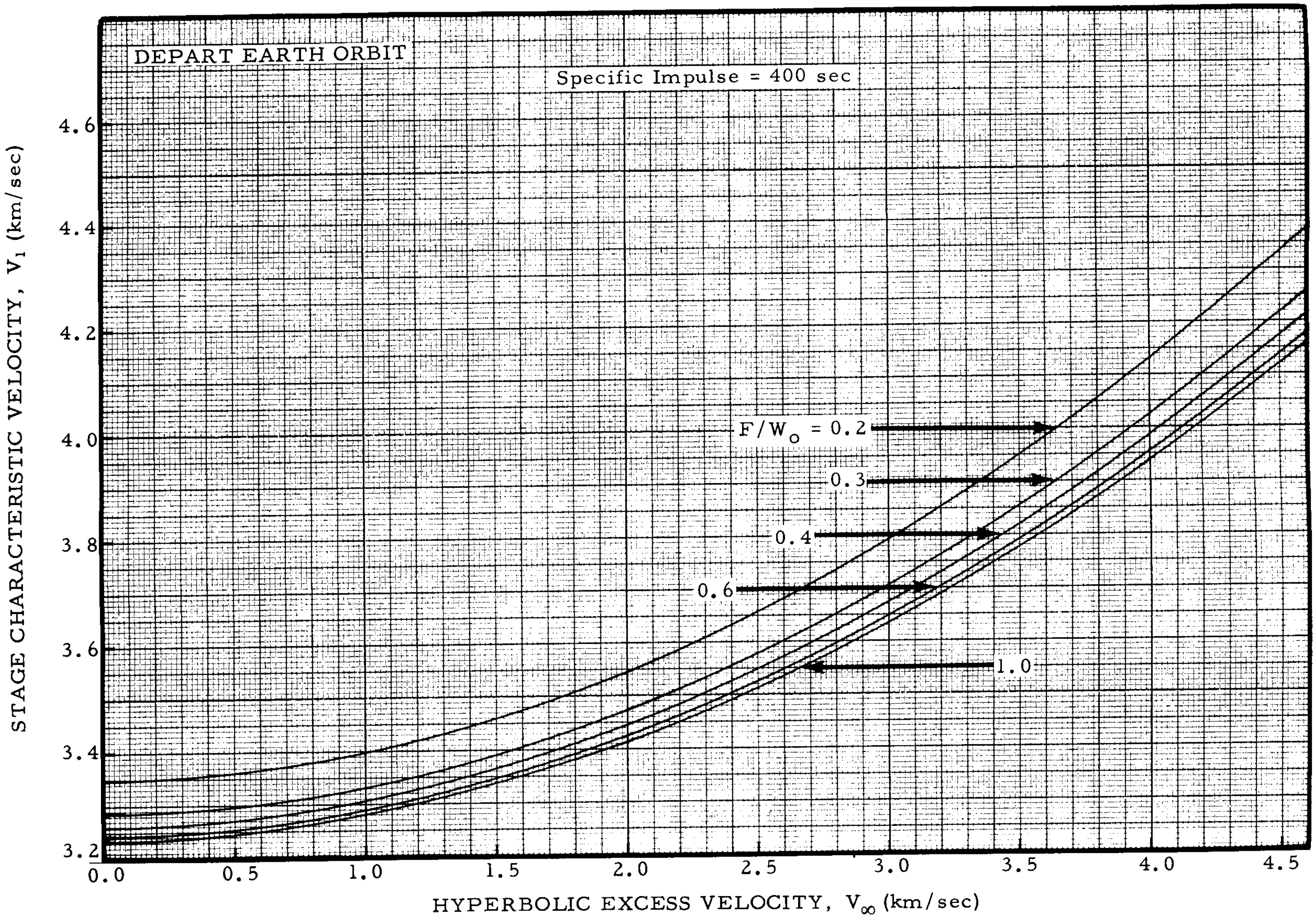

FIGURE 5a. CHARACTERISTIC VELOCITY, V_1 (km/sec), VERSUS HYPERBOLIC EXCESS VELOCITY, V_∞ (km/sec), WITH THRUST-TO-WEIGHT RATIO AS A PARAMETER FOR A CONSTANT SPECIFIC IMPULSE OF 400 SECONDS

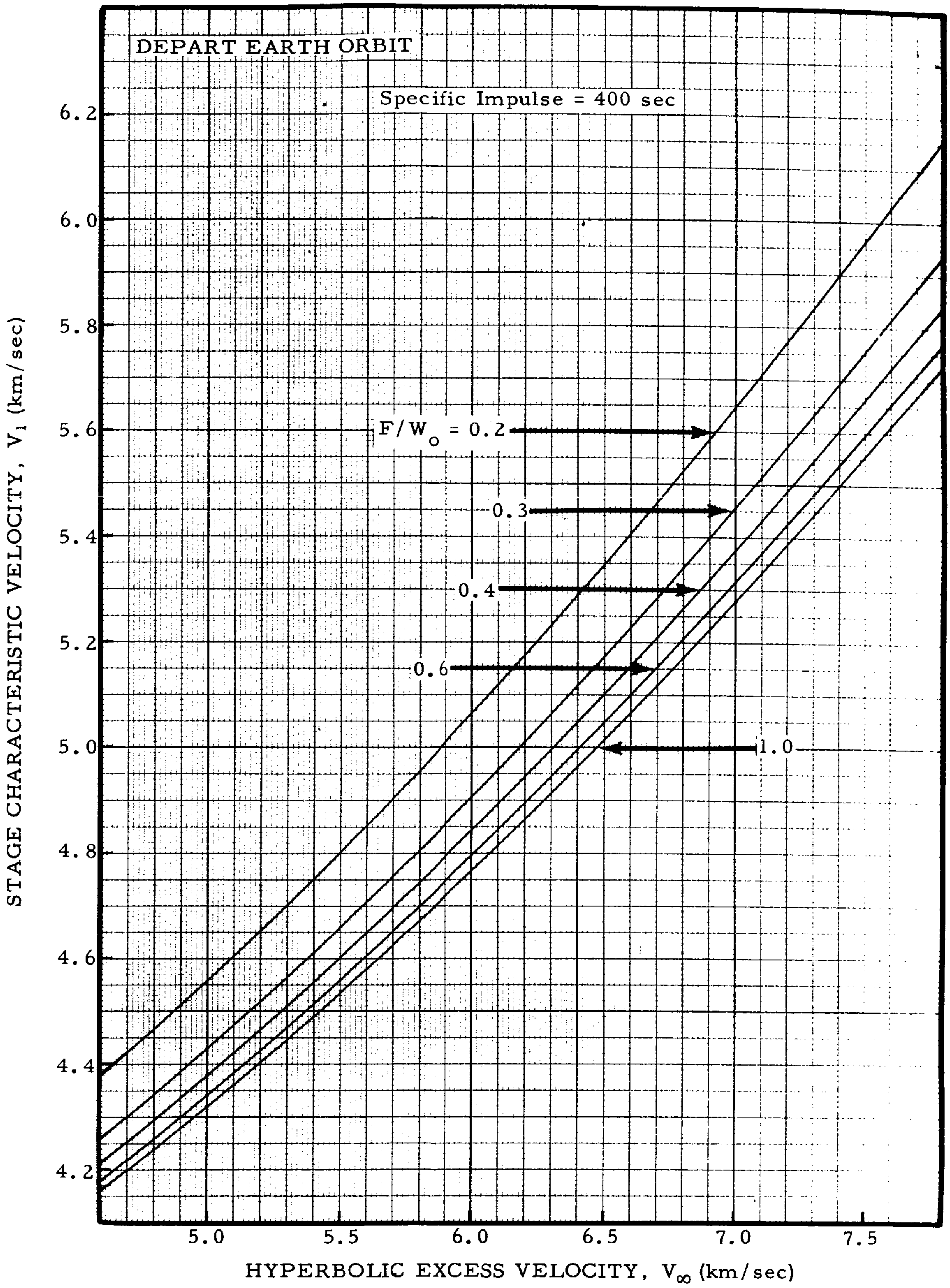

FIGURE 5b. CHARACTERISTIC VELOCITY, V_1 (km/sec), VERSUS HYPERBOLIC EXCESS VELOCITY, V_∞ (km/sec), WITH THRUST-TO-WEIGHT RATIO AS A PARAMETER FOR A CONSTANT SPECIFIC IMPULSE OF 400 SECONDS

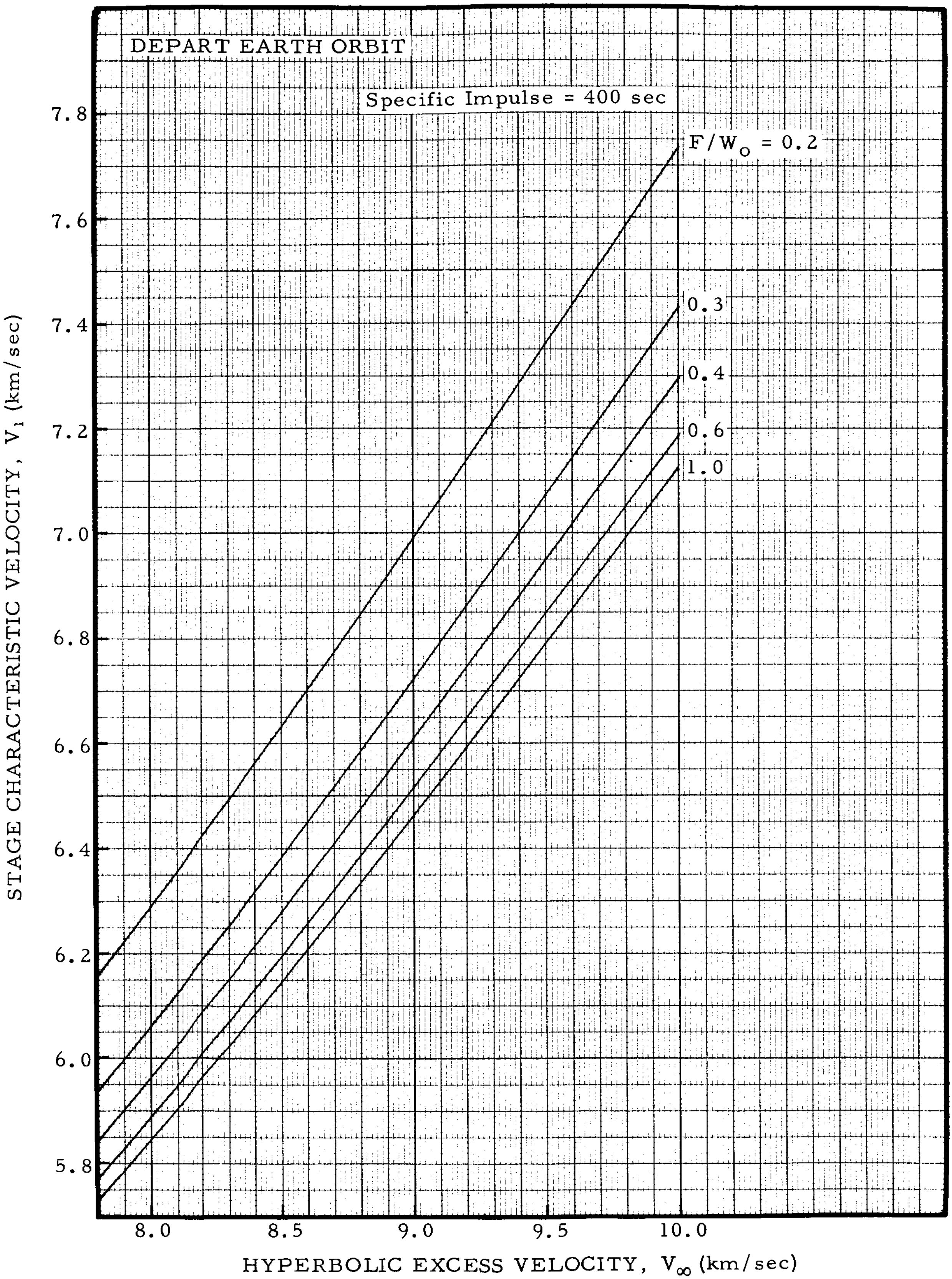

FIGURE 5c. CHARACTERISTIC VELOCITY, V_1 (km/sec), VERSUS HYPERBOLIC EXCESS VELOCITY, V_∞ (km/sec), WITH THRUST-TO-WEIGHT RATIO AS A PARAMETER FOR A CONSTANT SPECIFIC IMPULSE OF 400 SECONDS

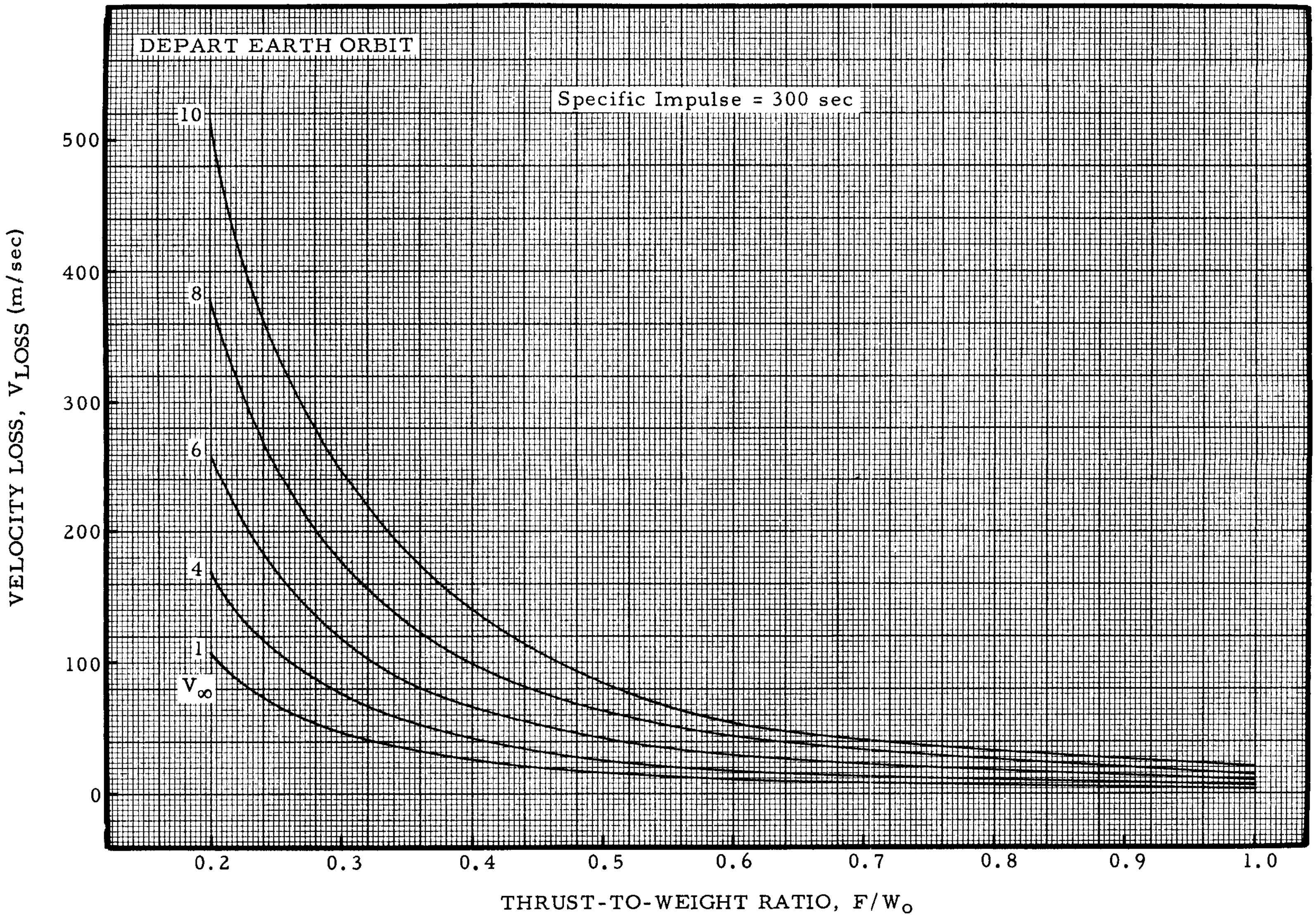

FIGURE 6. VELOCITY LOSS (m/sec) DUE TO GRAVITY VERSUS THRUST-TO-WEIGHT RATIO WITH HYPERBOLIC EXCESS VELOCITY, V_∞ (km/sec), AS A PARAMETER FOR A CONSTANT SPECIFIC IMPULSE OF 300 SECONDS

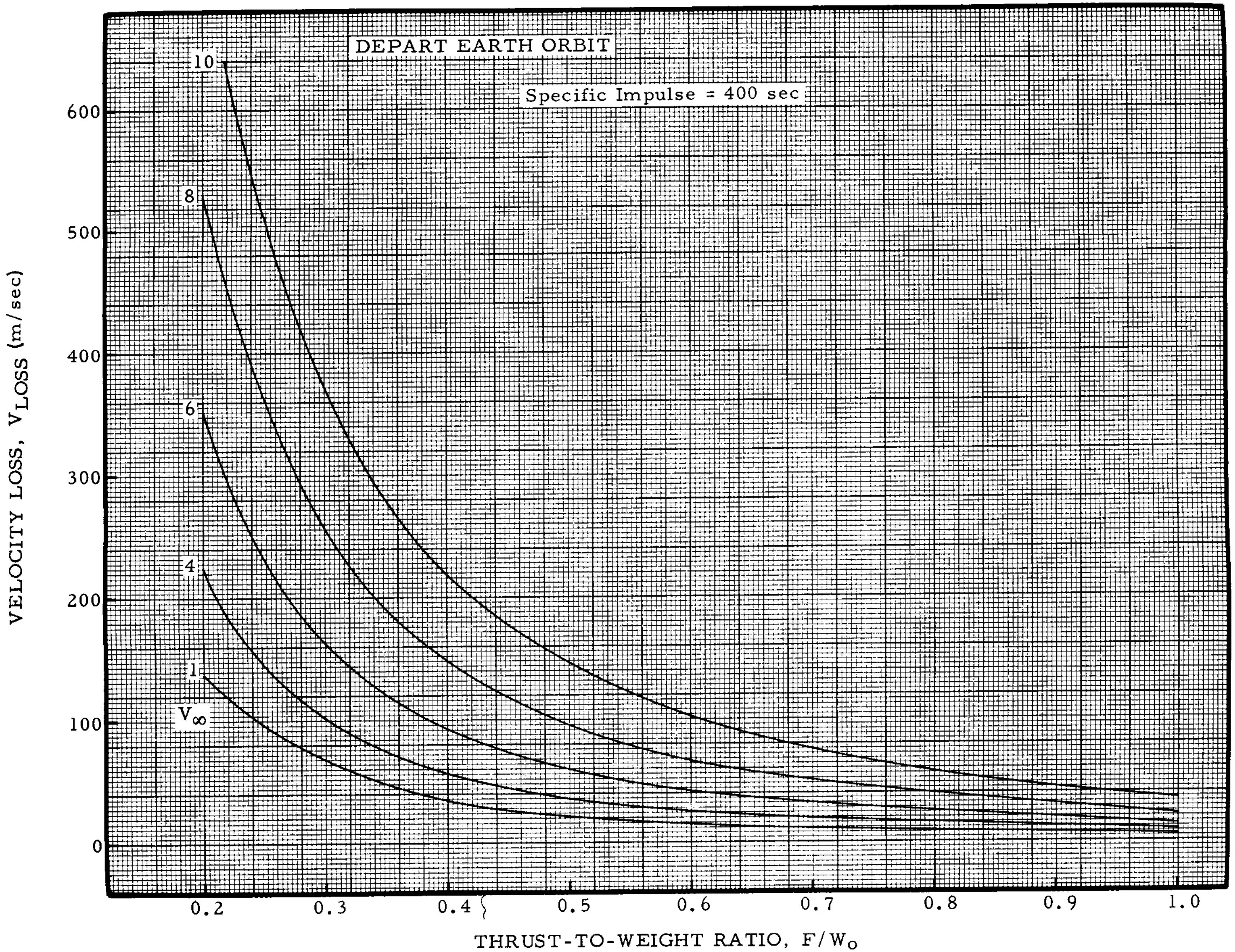

FIGURE 7. VELOCITY LOSS (m/sec) DUE TO GRAVITY VERSUS THRUST-TO-WEIGHT RATIO WITH HYPERBOLIC EXCESS VELOCITY, V_∞ (km/sec), AS A PARAMETER FOR A CONSTANT SPECIFIC IMPULSE OF 400 SECONDS

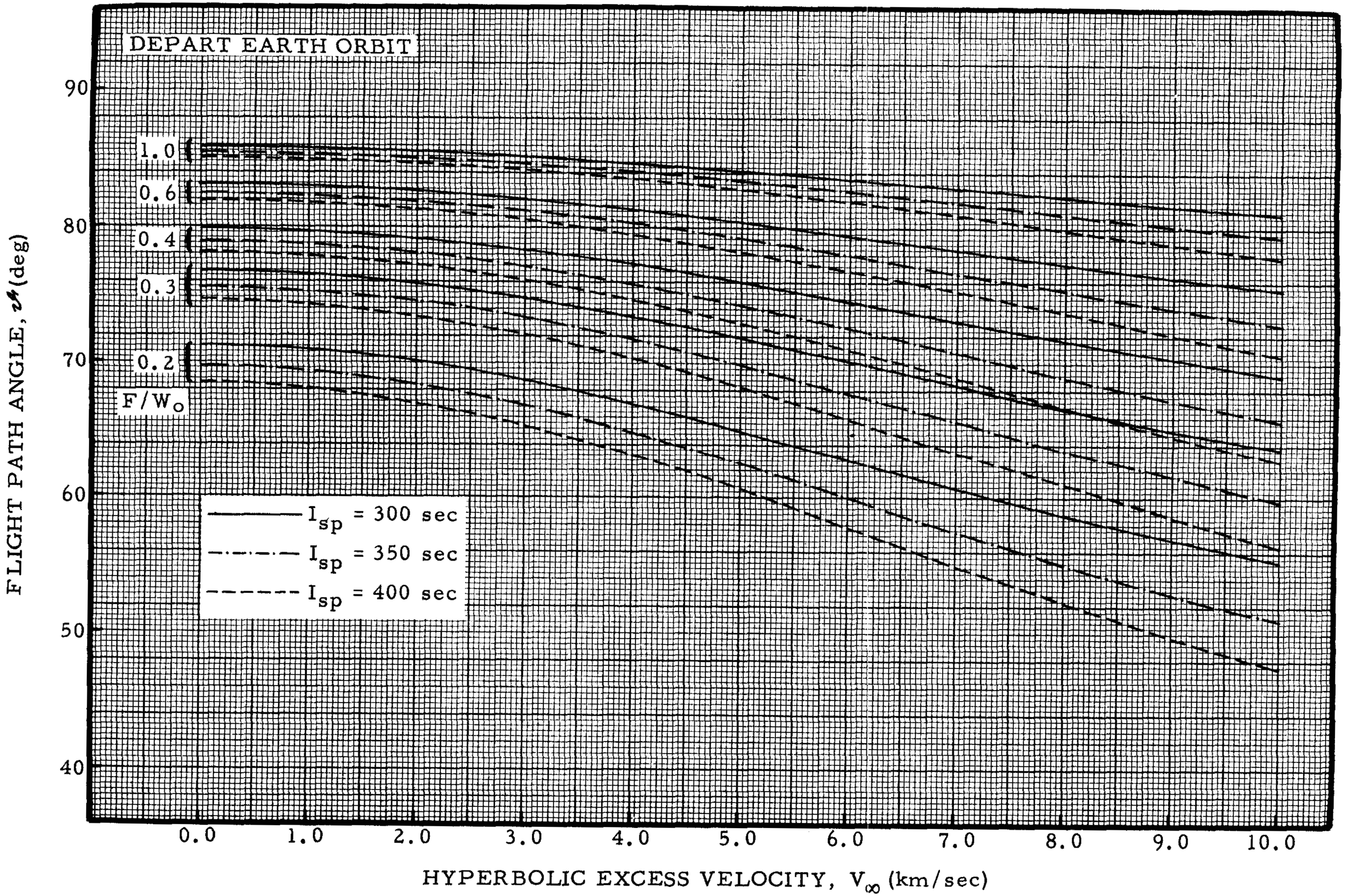

FIGURE 8. FLIGHT PATH ANGLE (deg) VERSUS HYPERBOLIC EXCESS VELOCITY (km/sec) WITH THRUST-TO-WEIGHT RATIO AS A PARAMETER

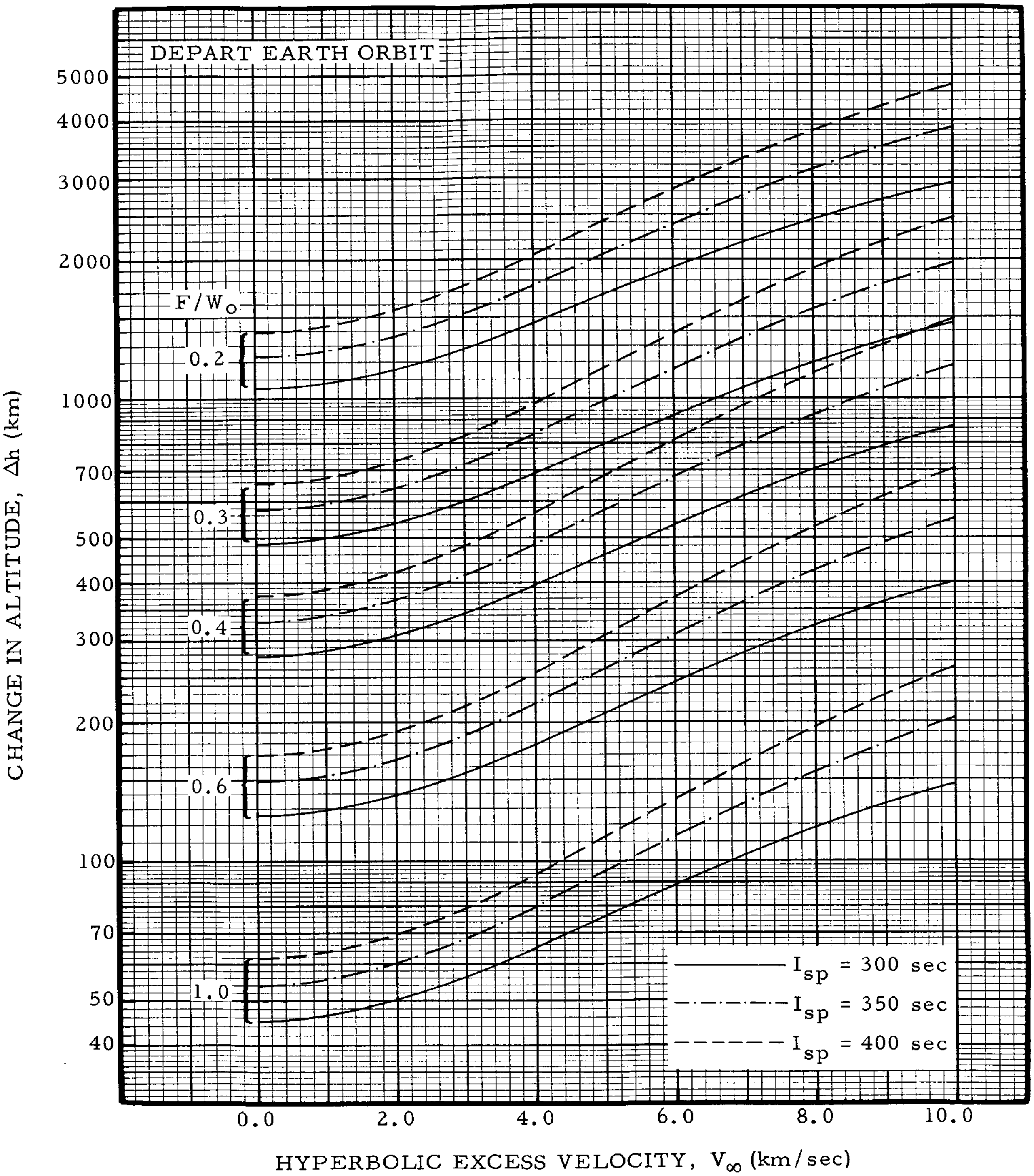

FIGURE 9. CHANGE IN ALTITUDE (km) VERSUS HYPERBOLIC EXCESS VELOCITY (km/sec) WITH THRUST-TO-WEIGHT RATIO AS A PARAMETER

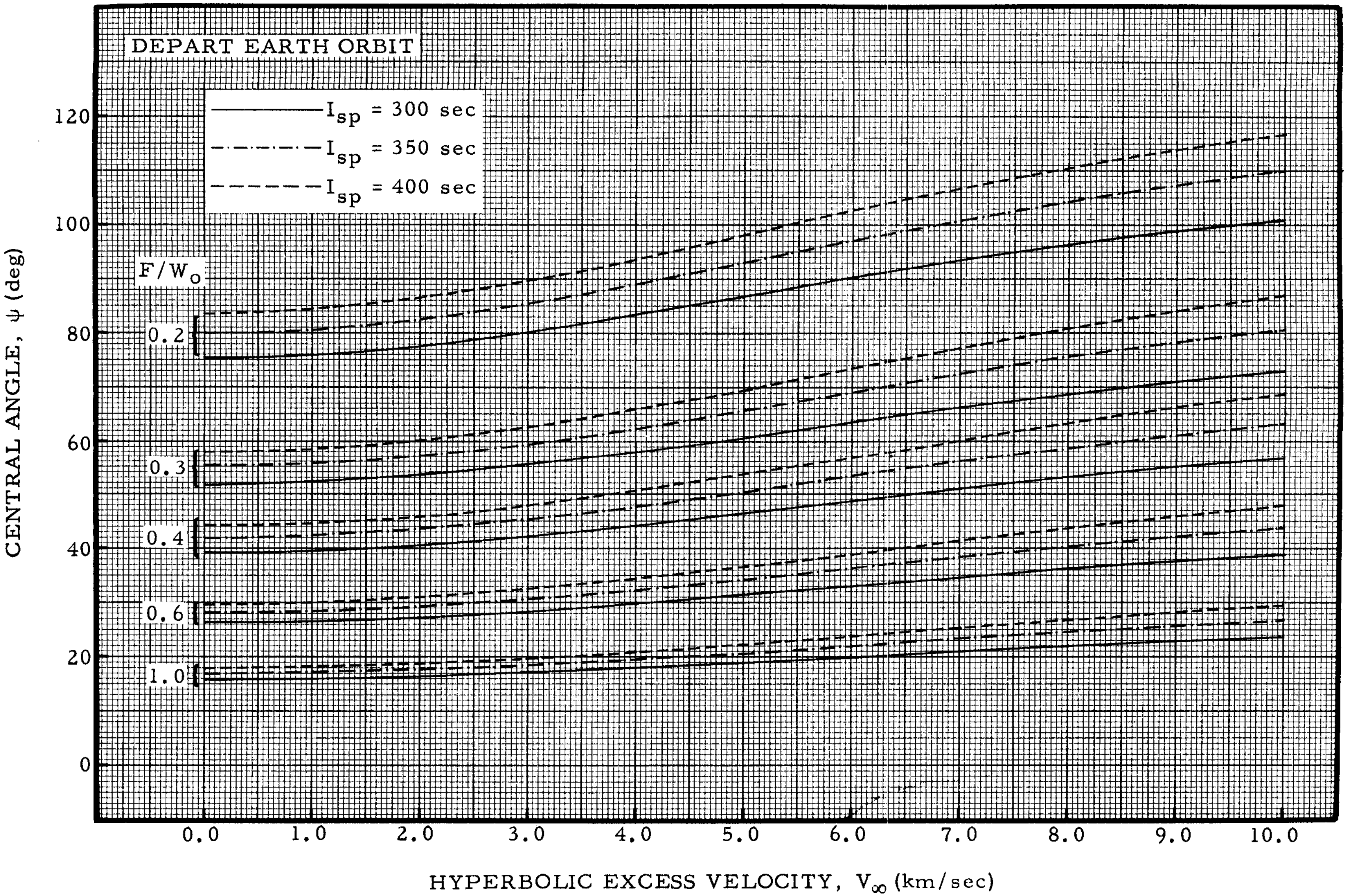

FIGURE 10. CENTRAL ANGLE (deg) VERSUS HYPERBOLIC EXCESS VELOCITY (km/sec) WITH THRUST-TO-WEIGHT RATIO AS A PARAMETER

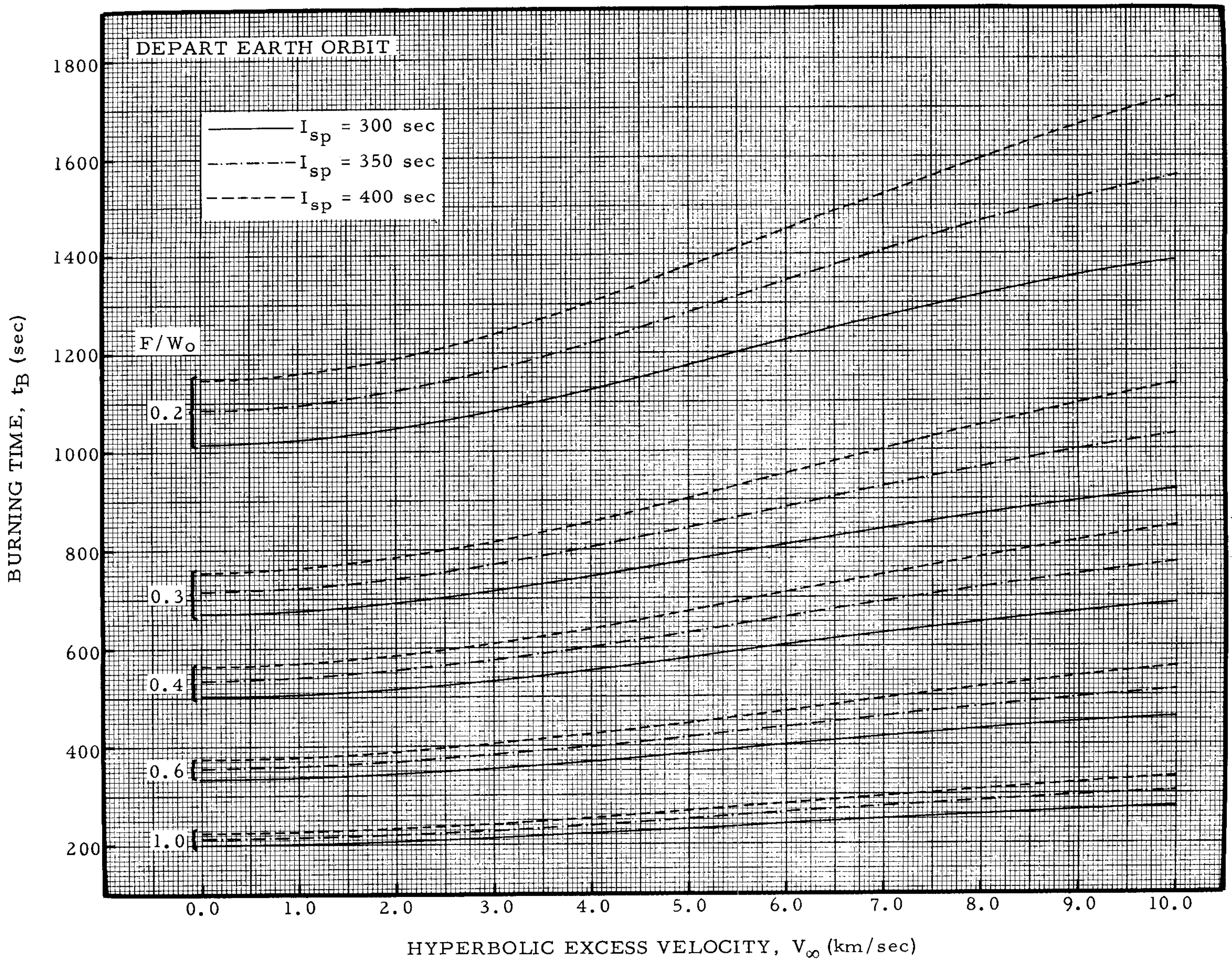

FIGURE 11. BURNING TIME (sec) VERSUS HYPERBOLIC EXCESS VELOCITY (km/sec) WITH THRUST-TO-WEIGHT RATIO AS A PARAMETER

BRAKE TO EARTH ORBIT

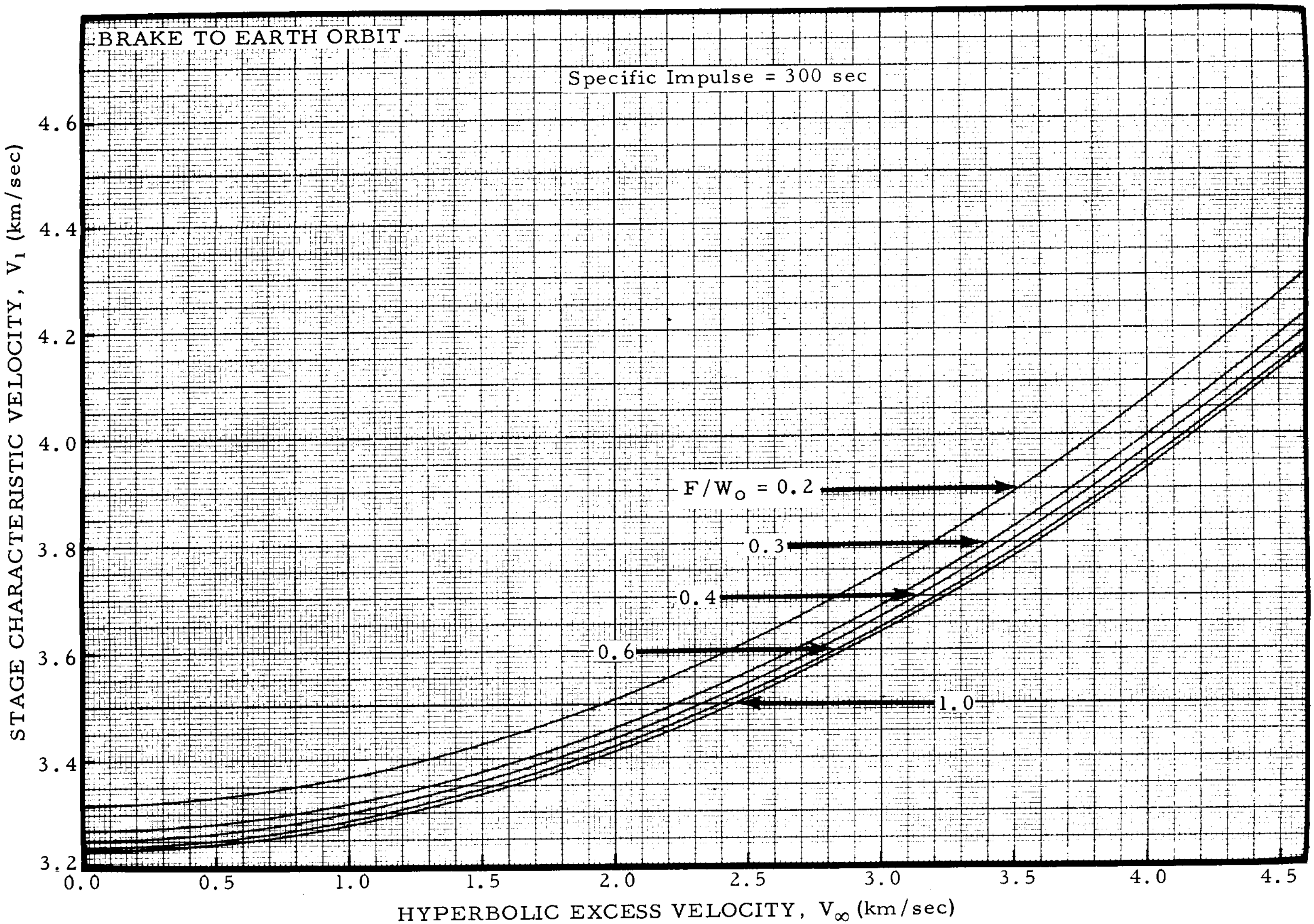

FIGURE 1a. CHARACTERISTIC VELOCITY, V_1 (km/sec), VERSUS HYPERBOLIC EXCESS VELOCITY, V_∞ (km/sec), WITH THRUST-TO-WEIGHT RATIO AS A PARAMETER FOR A CONSTANT SPECIFIC IMPULSE OF 300 SECONDS

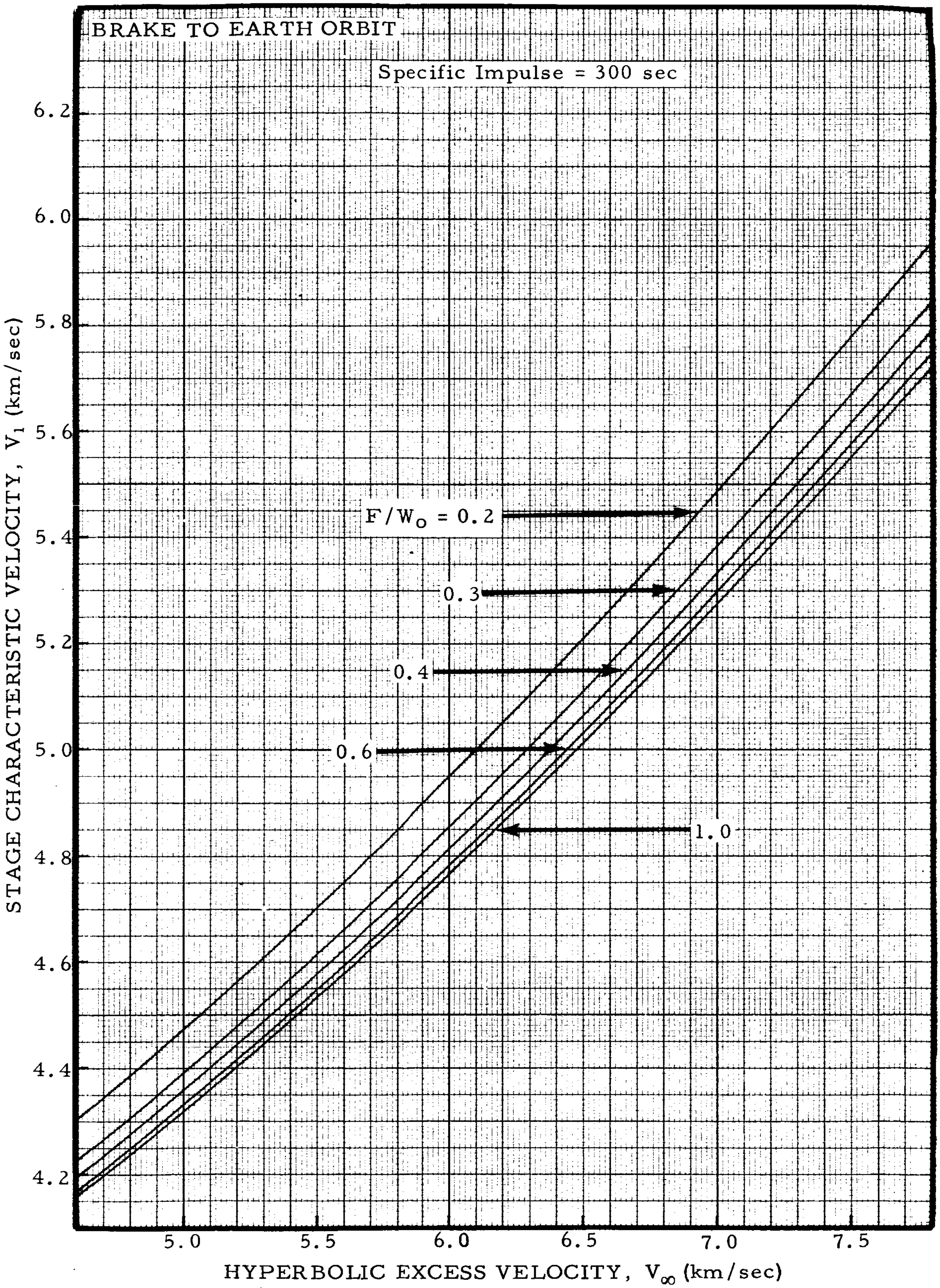

FIGURE 1b. CHARACTERISTIC VELOCITY, V_1 (km/sec), VERSUS HYPERBOLIC EXCESS VELOCITY, V_∞ (km/sec), WITH THRUST-TO-WEIGHT RATIO AS A PARAMETER FOR A CONSTANT SPECIFIC IMPULSE OF 300 SECONDS

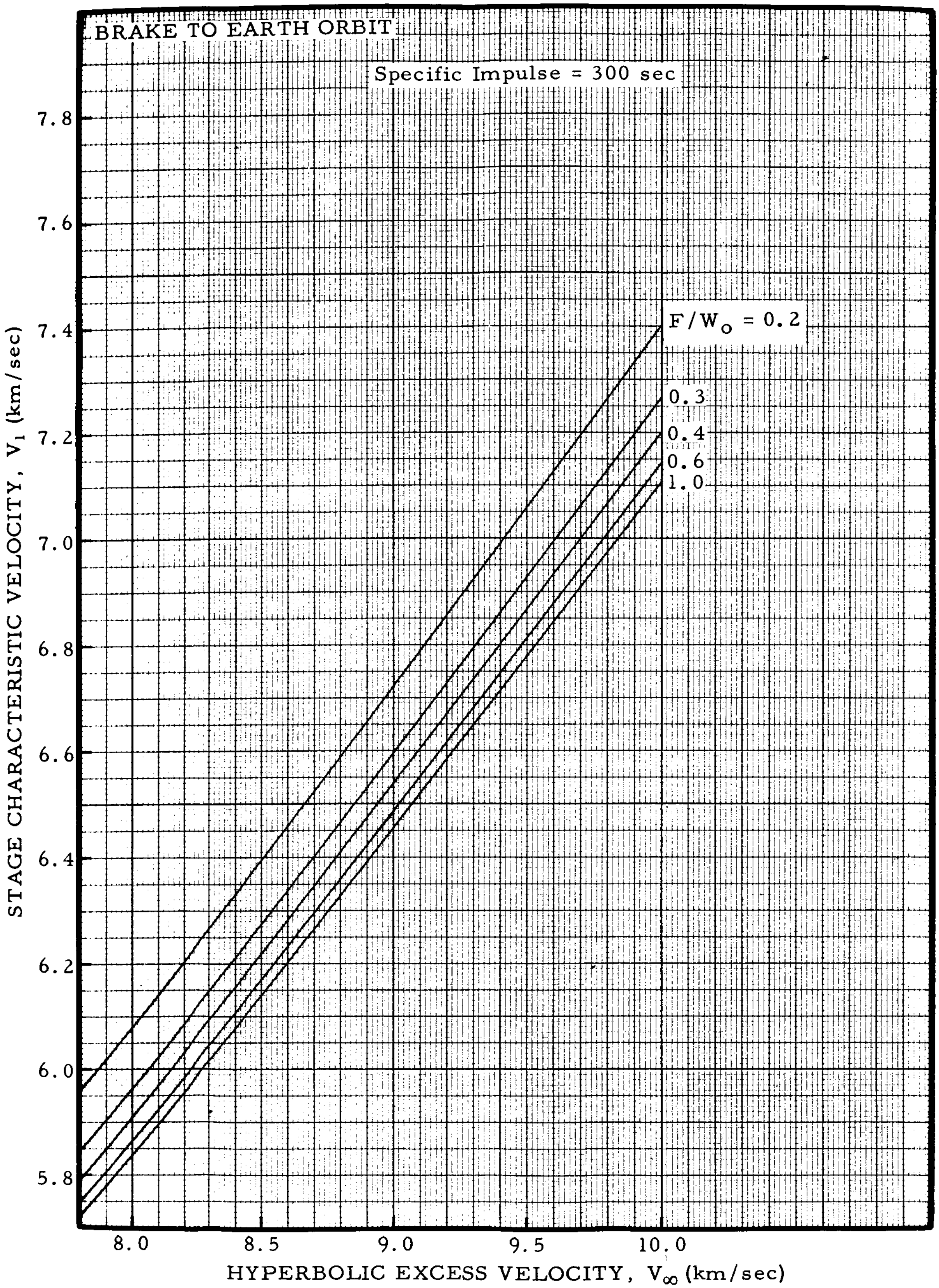

FIGURE 1c. CHARACTERISTIC VELOCITY, V_1 (km/sec), VERSUS HYPERBOLIC EXCESS VELOCITY, V_∞ (km/sec), WITH THRUST-TO-WEIGHT RATIO AS A PARAMETER FOR A CONSTANT SPECIFIC IMPULSE OF 300 SECONDS

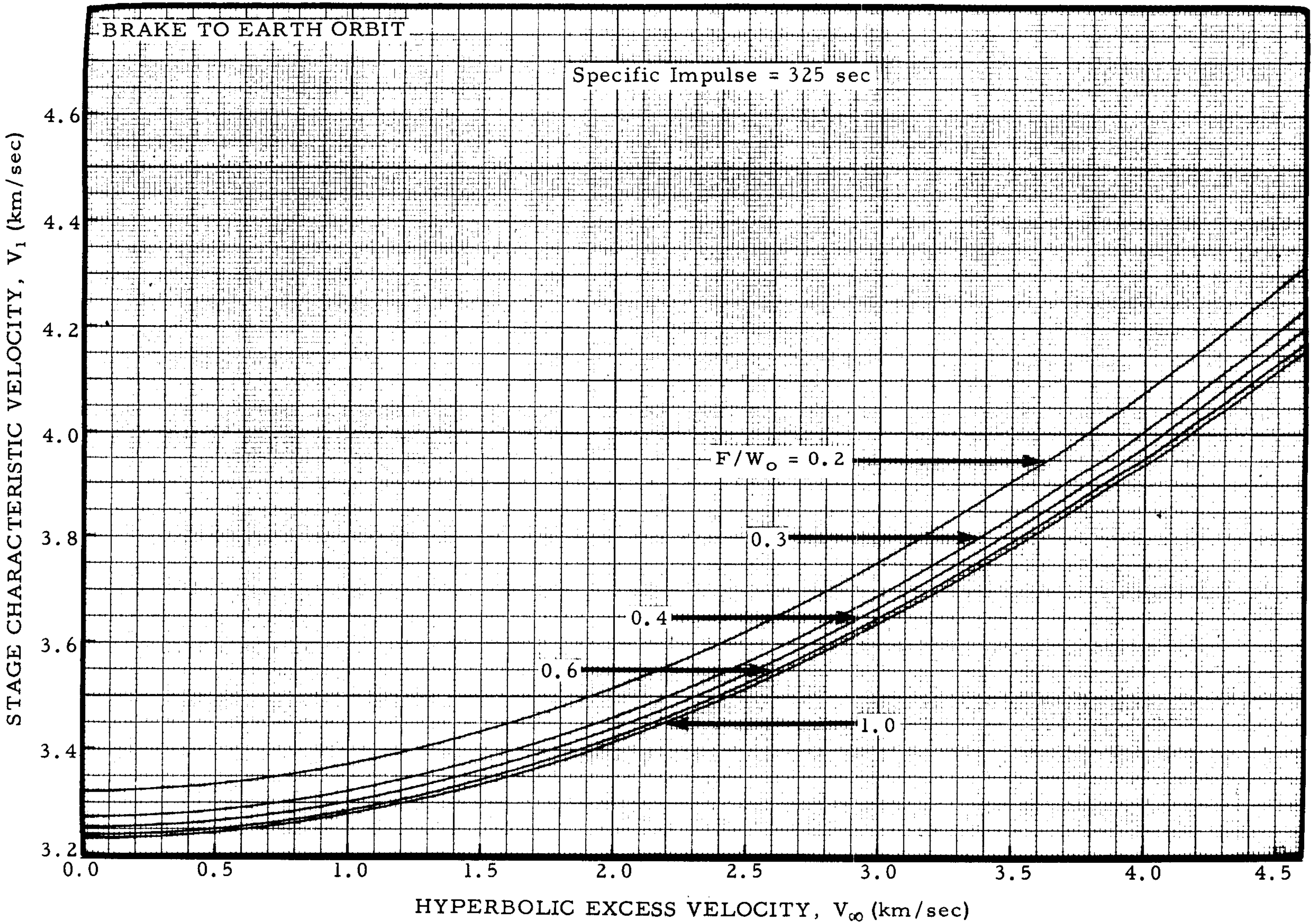

FIGURE 2a. CHARACTERISTIC VELOCITY, V_1 (km/sec), VERSUS HYPERBOLIC EXCESS VELOCITY, V_∞ (km/sec), WITH THRUST-TO-WEIGHT RATIO AS A PARAMETER FOR A CONSTANT SPECIFIC IMPULSE OF 325 SECONDS

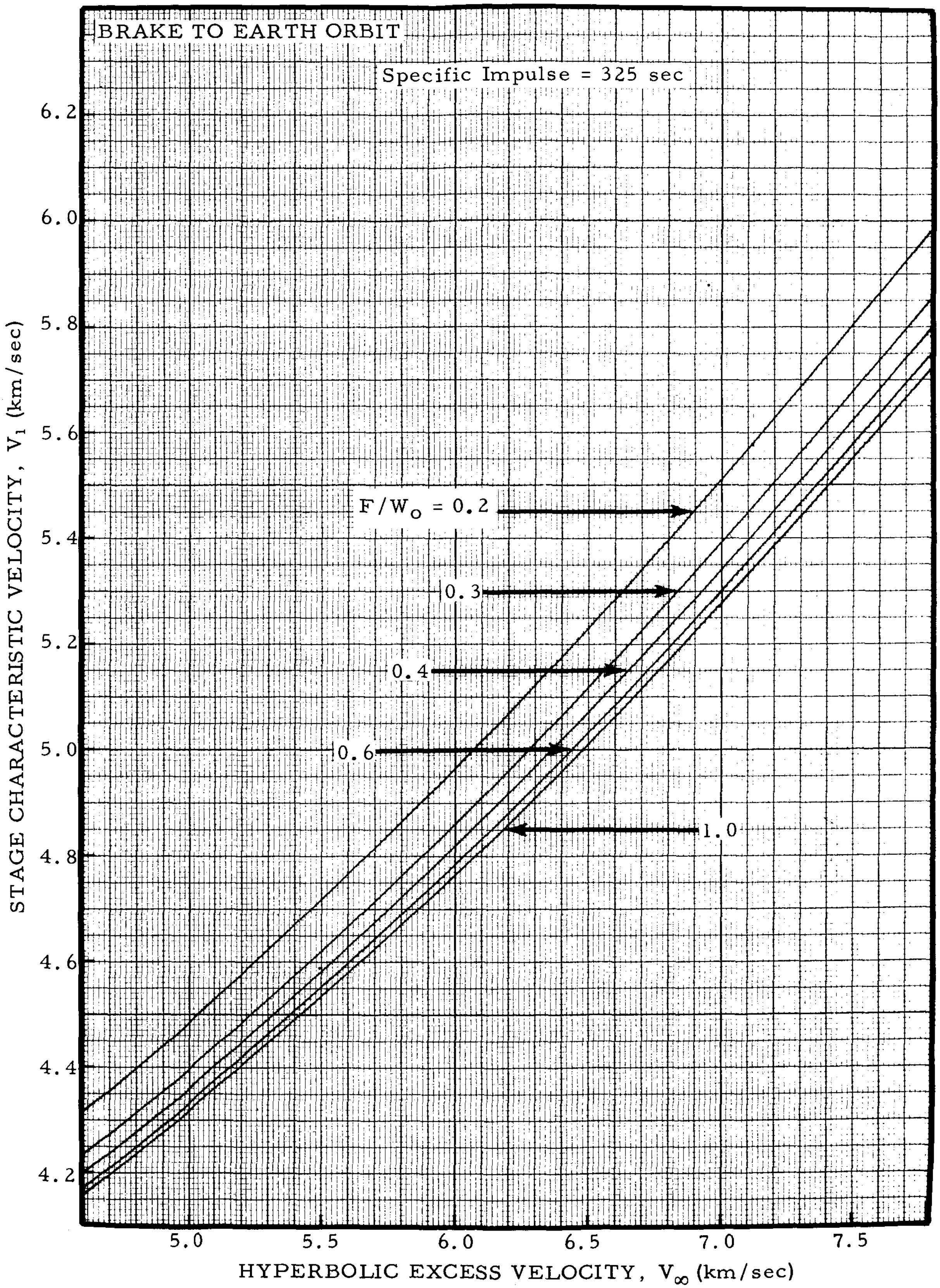

FIGURE 2b. CHARACTERISTIC VELOCITY, V_1 (km/sec), VERSUS HYPERBOLIC EXCESS VELOCITY, V_∞ (km/sec), WITH THRUST-TO-WEIGHT RATIO AS A PARAMETER FOR A CONSTANT SPECIFIC IMPULSE OF 325 SECONDS

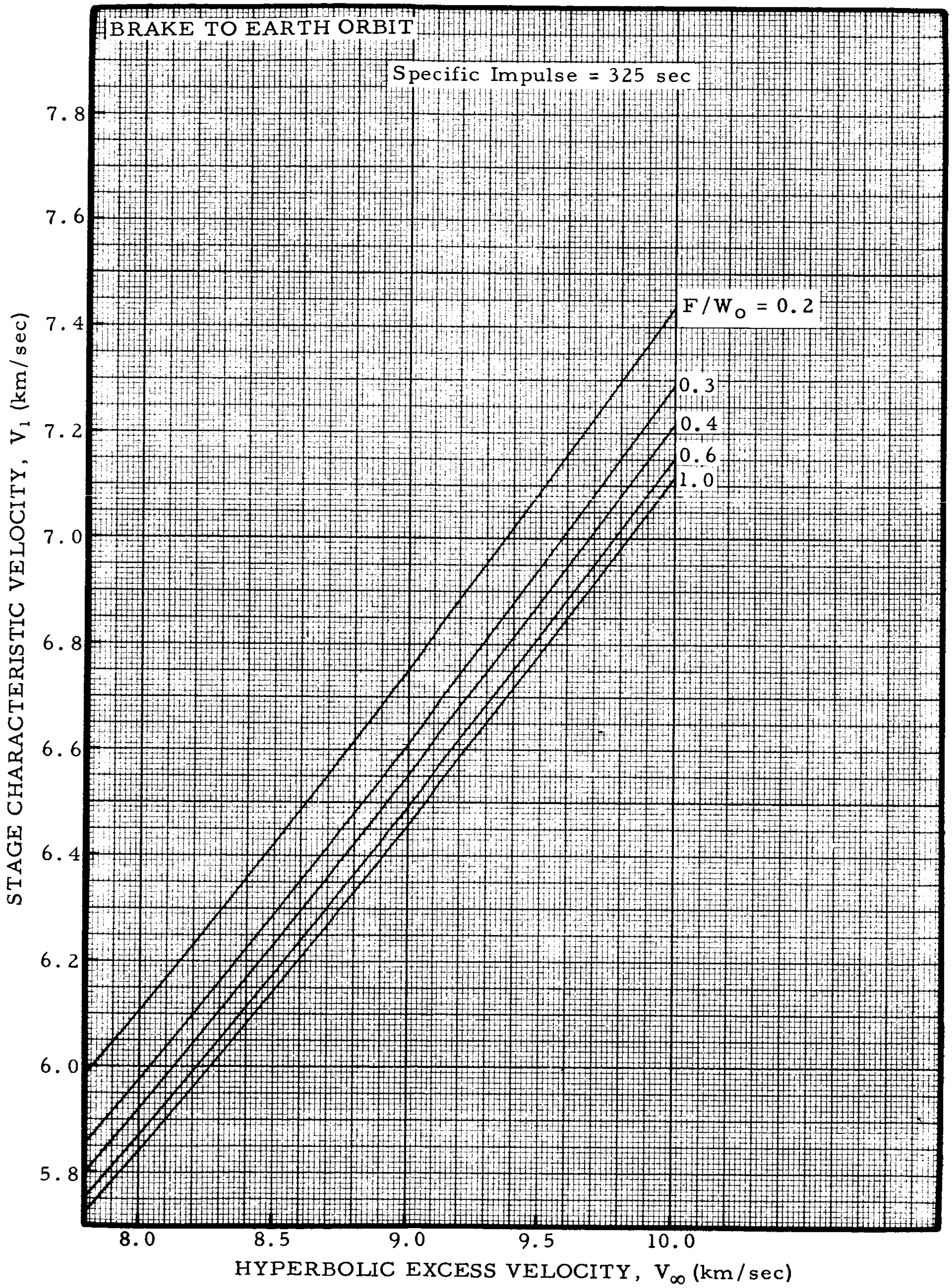

FIGURE 2c. CHARACTERISTIC VELOCITY, V_1 (km/sec), VERSUS HYPERBOLIC EXCESS VELOCITY, V_∞ (km/sec), WITH THRUST-TO-WEIGHT RATIO AS A PARAMETER FOR A CONSTANT SPECIFIC IMPULSE OF 325 SECONDS

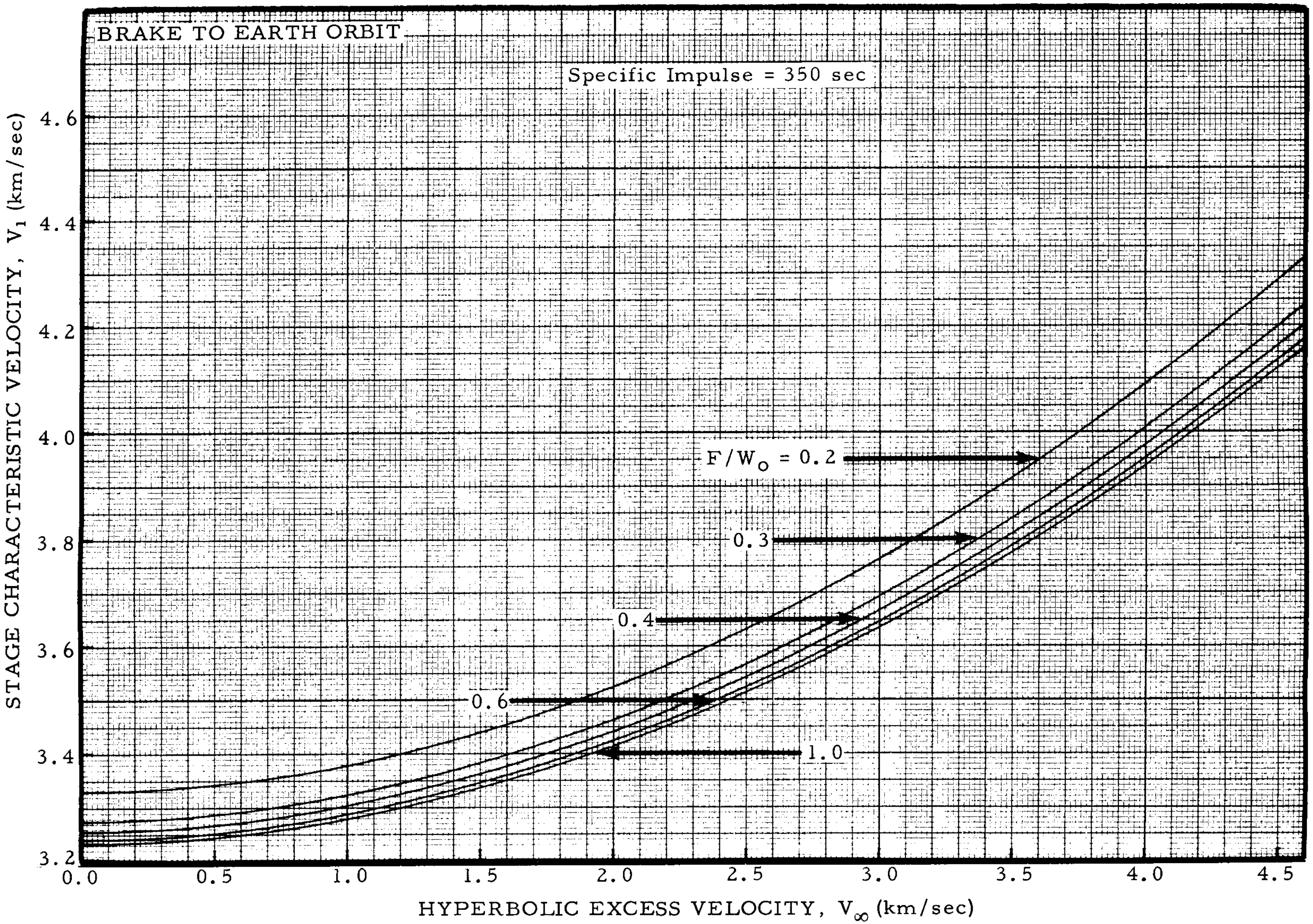

FIGURE 3a. CHARACTERISTIC VELOCITY, V_1 (km/sec), VERSUS HYPERBOLIC EXCESS VELOCITY, V_∞ (km/sec), WITH THRUST-TO-WEIGHT RATIO AS A PARAMETER FOR A CONSTANT SPECIFIC IMPULSE OF 350 SECONDS

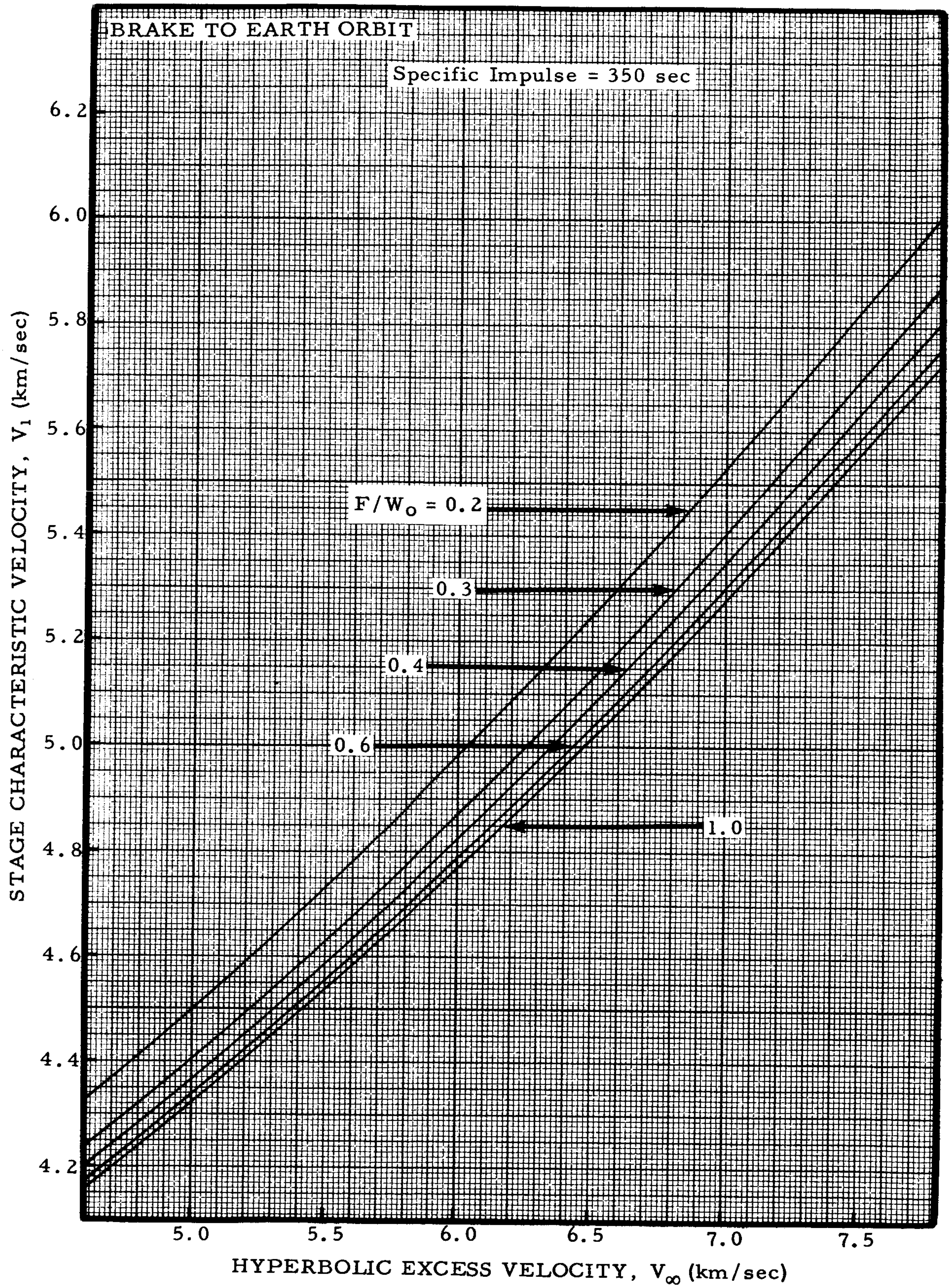

FIGURE 3b. CHARACTERISTIC VELOCITY, V_1 (km/sec), VERSUS HYPERBOLIC EXCESS VELOCITY, V_∞ (km/sec), WITH THRUST-TO-WEIGHT RATIO AS A PARAMETER FOR A CONSTANT SPECIFIC IMPULSE OF 350 SECONDS

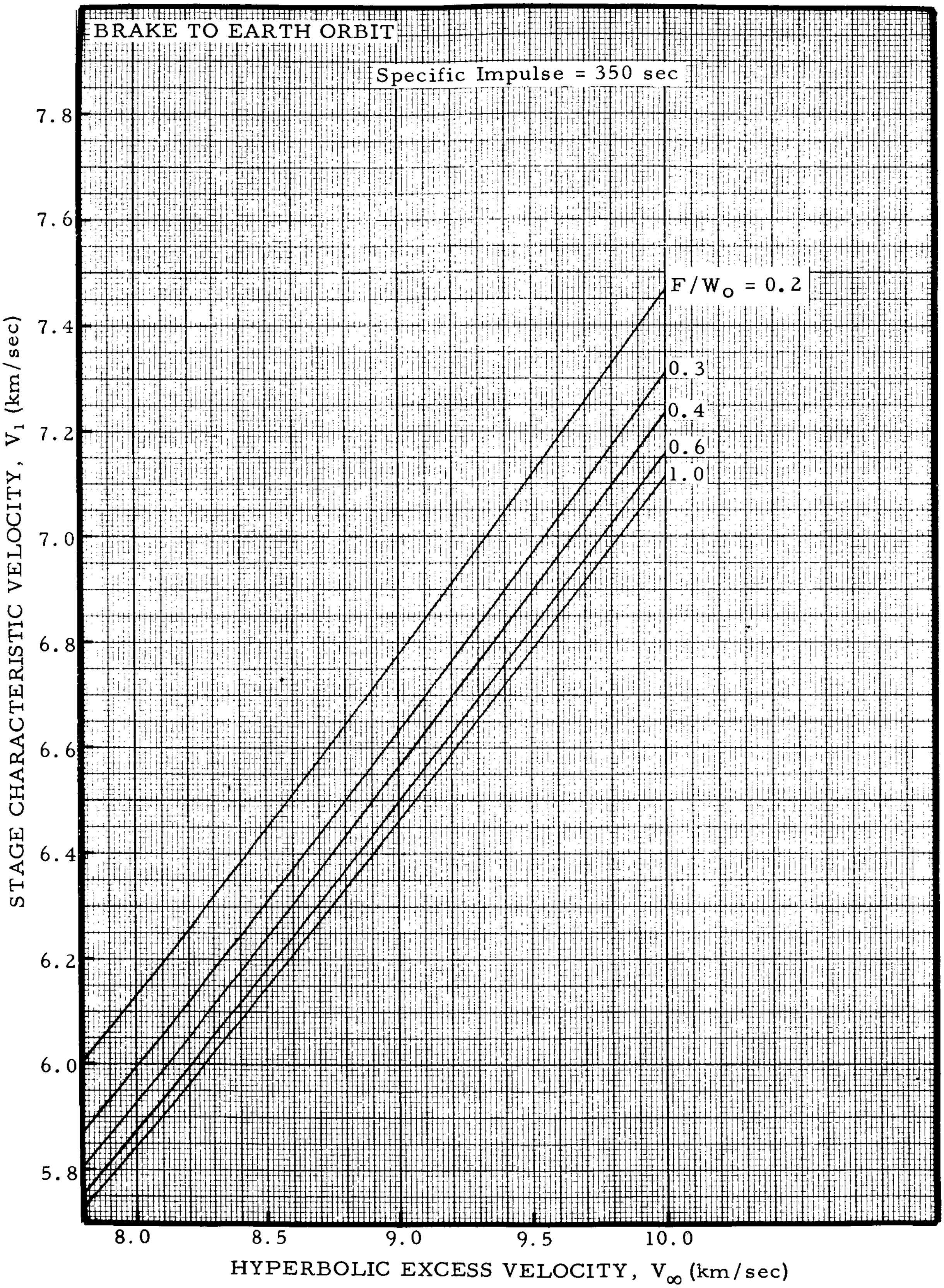

FIGURE 3c. CHARACTERISTIC VELOCITY, V_1 (km/sec), VERSUS HYPERBOLIC EXCESS VELOCITY, V_∞ (km/sec), WITH THRUST-TO-WEIGHT RATIO AS A PARAMETER FOR A CONSTANT SPECIFIC IMPULSE OF 350 SECONDS

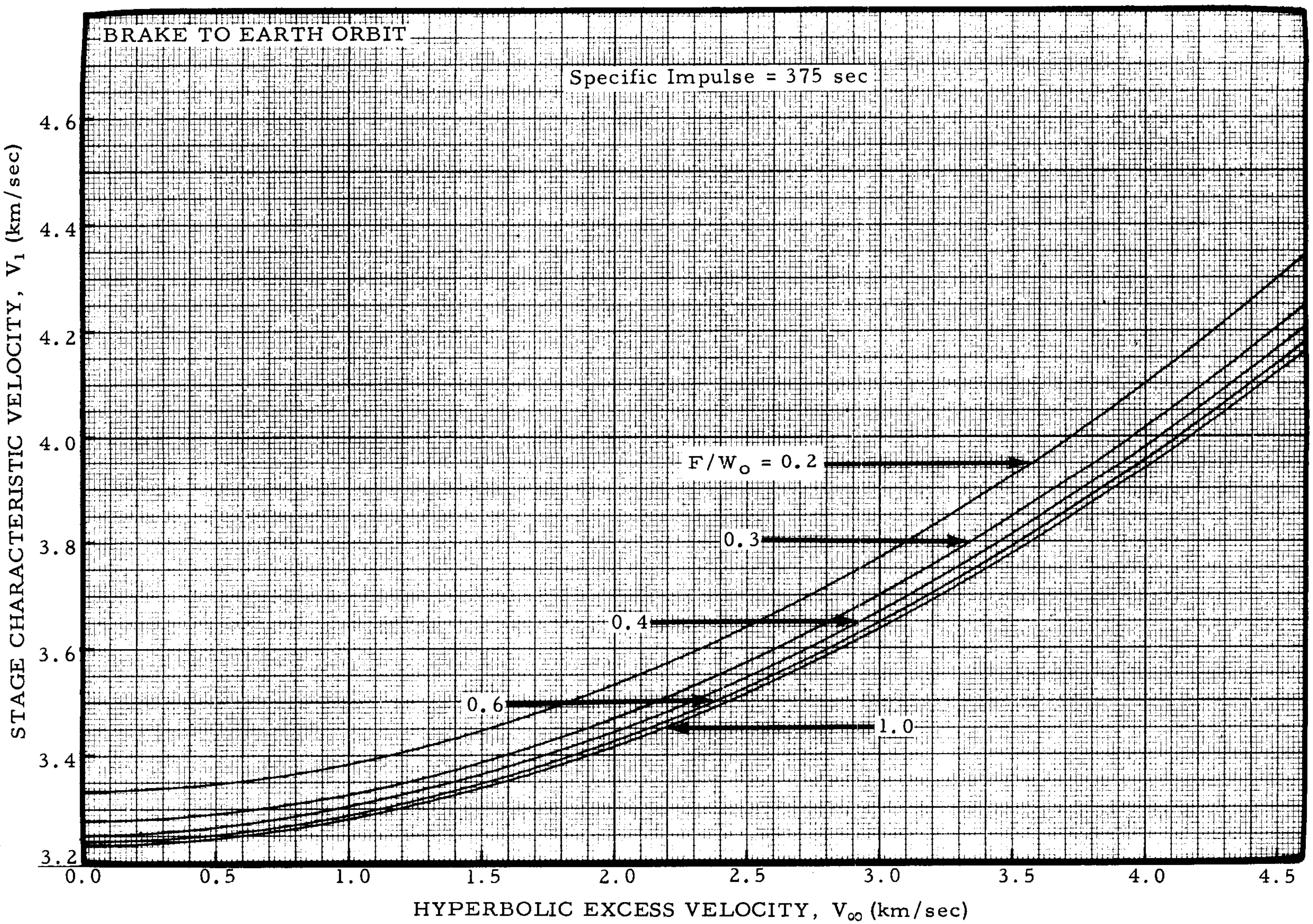

FIGURE 4a. CHARACTERISTIC VELOCITY, V_1 (km/sec), VERSUS HYPERBOLIC EXCESS VELOCITY, V_∞ (km/sec), WITH THRUST-TO-WEIGHT RATIO AS A PARAMETER FOR A CONSTANT SPECIFIC IMPULSE OF 375 SECONDS

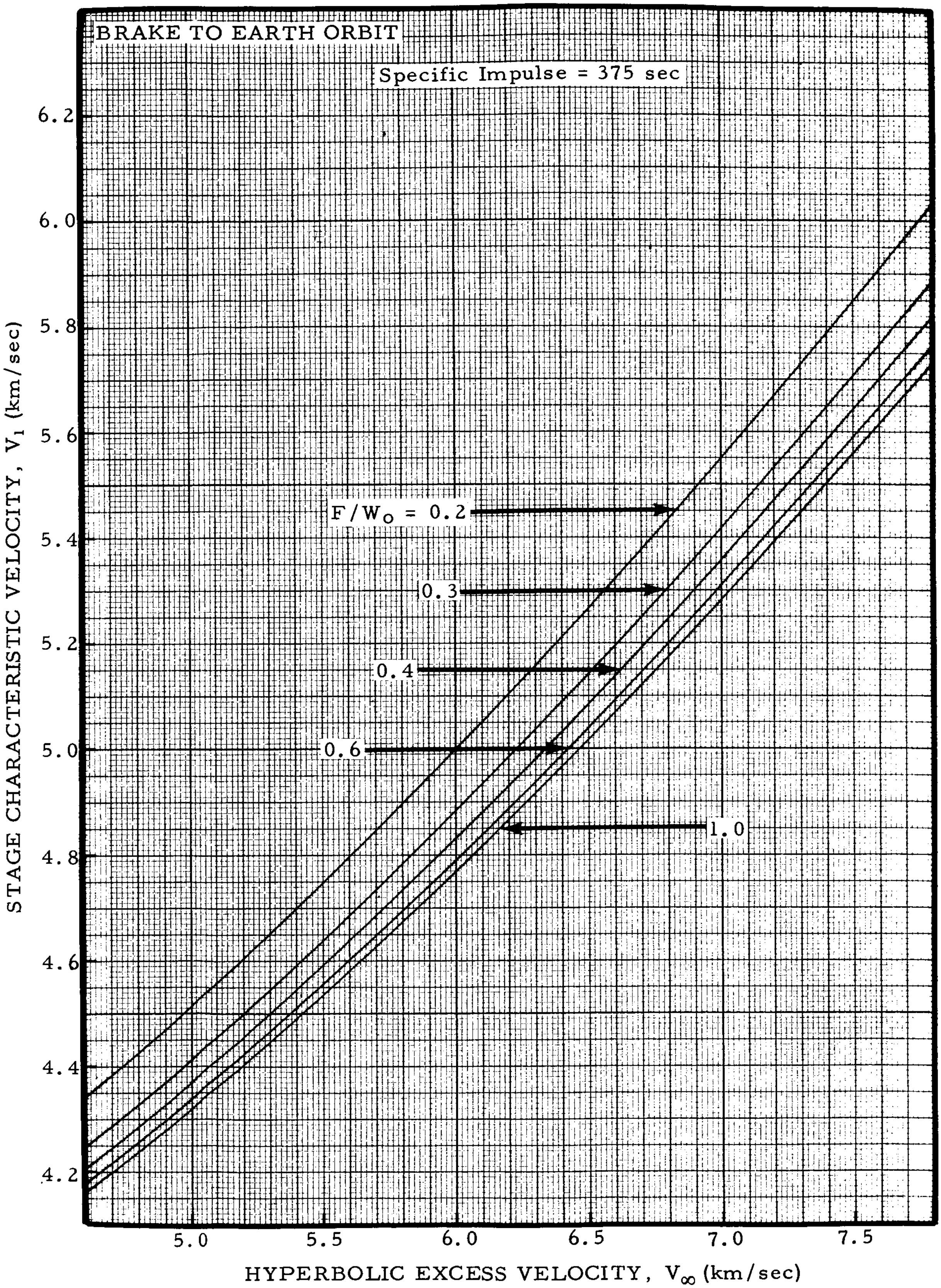

FIGURE 4b. CHARACTERISTIC VELOCITY, V_1 (km/sec), VERSUS HYPERBOLIC EXCESS VELOCITY, V_∞ (km/sec), WITH THRUST-TO-WEIGHT RATIO AS A PARAMETER FOR A CONSTANT SPECIFIC IMPULSE OF 375 SECONDS

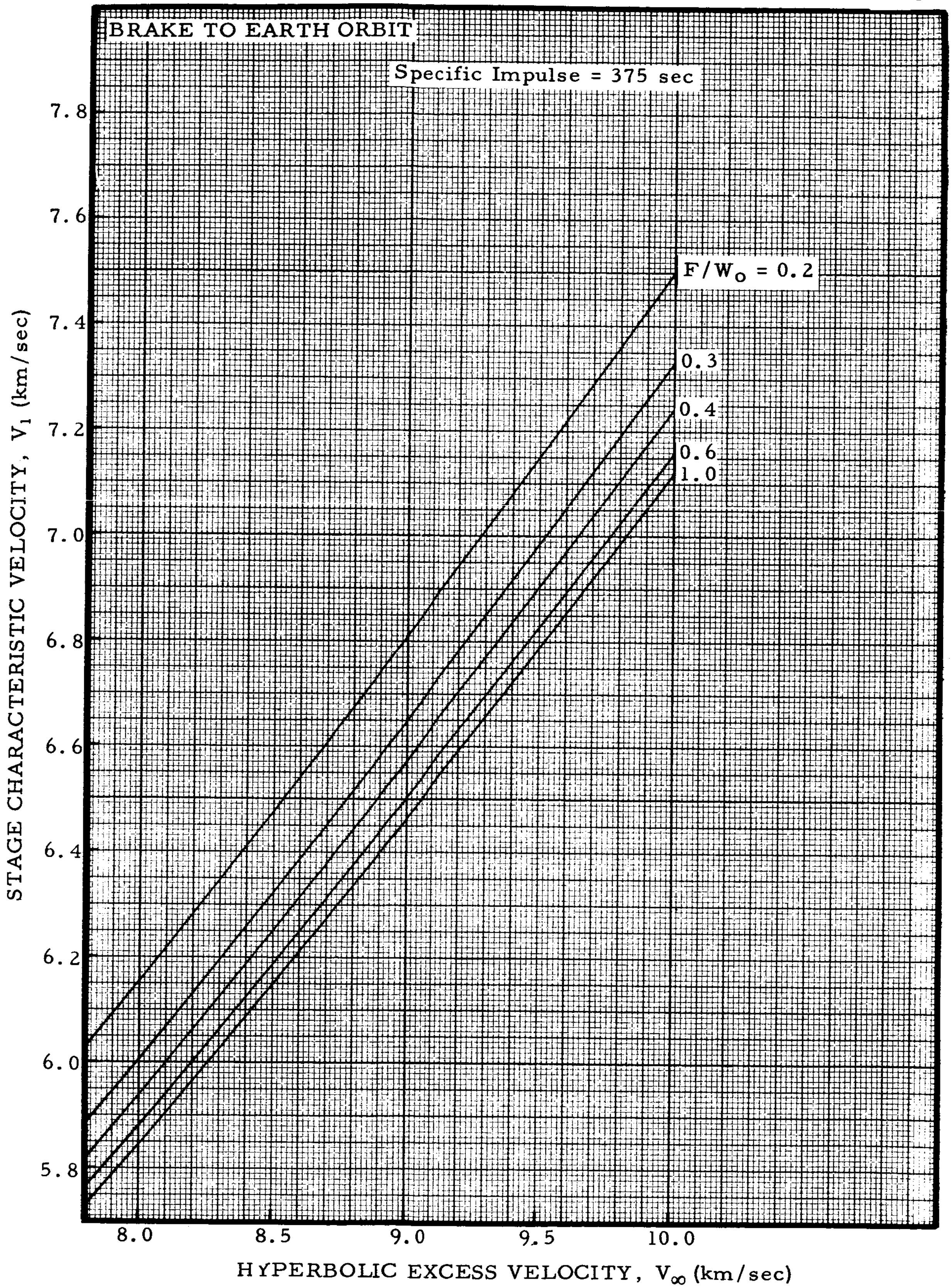

FIGURE 4c. CHARACTERISTIC VELOCITY, V_1 (km/sec), VERSUS HYPERBOLIC EXCESS VELOCITY, V_∞ (km/sec), WITH THRUST-TO-WEIGHT RATIO AS A PARAMETER FOR A CONSTANT SPECIFIC IMPULSE OF 375 SECONDS

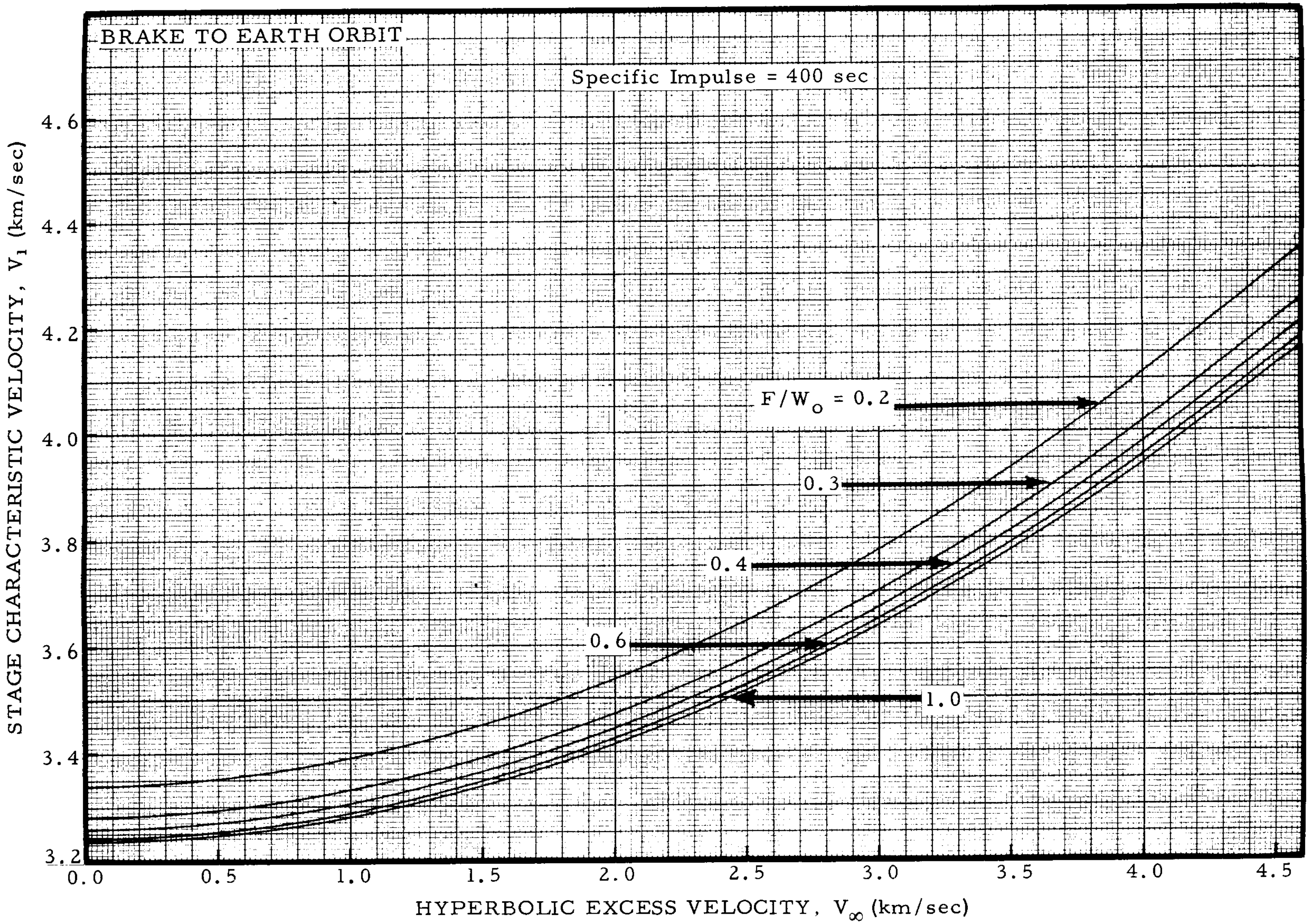

FIGURE 5a. CHARACTERISTIC VELOCITY, V_1 (km/sec), VERSUS HYPERBOLIC EXCESS VELOCITY, V_∞ (km/sec), WITH THRUST-TO-WEIGHT RATIO AS A PARAMETER FOR A CONSTANT SPECIFIC IMPULSE OF 400 SECONDS

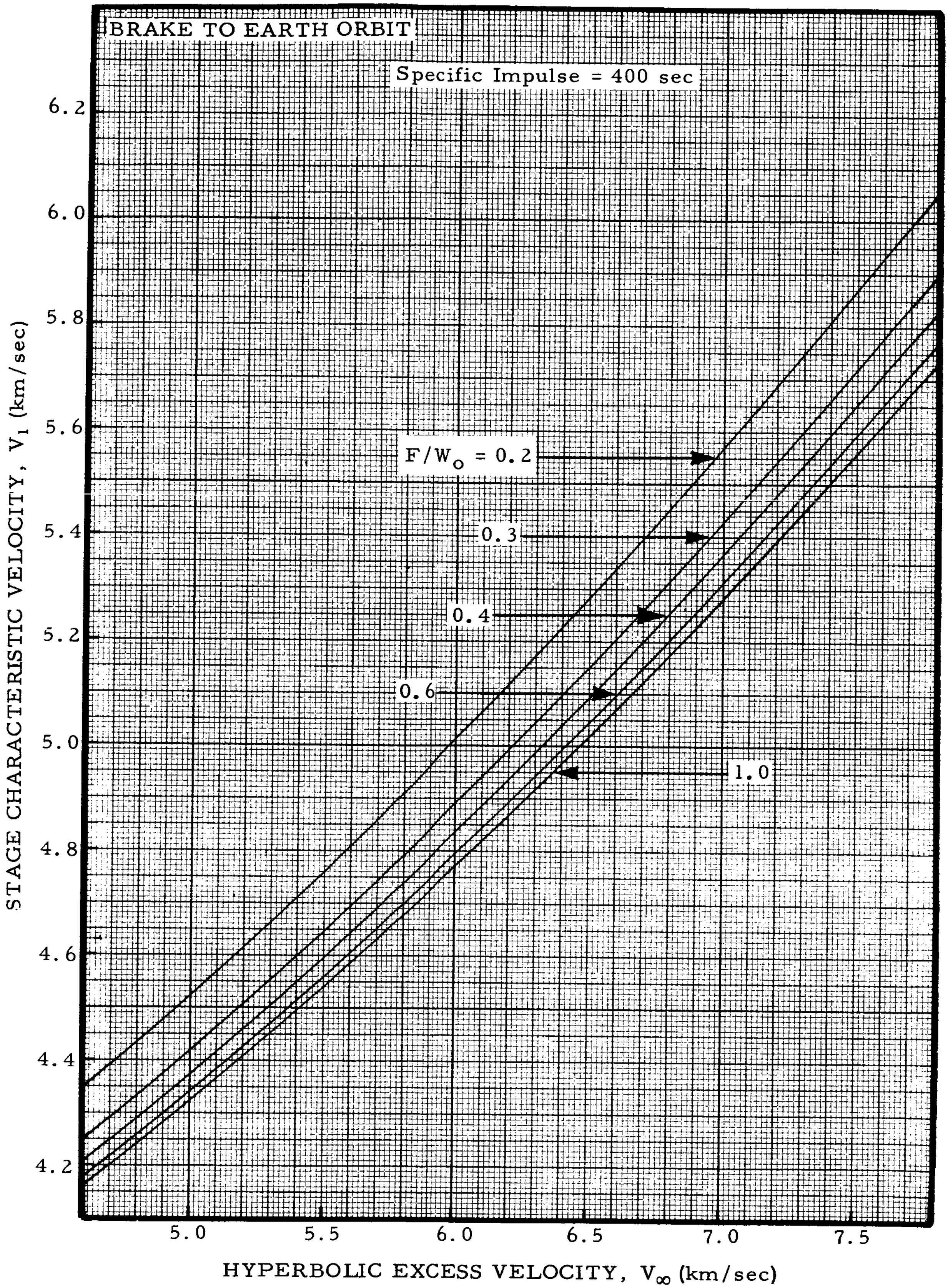

FIGURE 5b. CHARACTERISTIC VELOCITY, V_1 (km/sec), VERSUS HYPERBOLIC EXCESS VELOCITY, V_∞ (km/sec), WITH THRUST-TO-WEIGHT RATIO AS A PARAMETER FOR A CONSTANT SPECIFIC IMPULSE OF 400 SECONDS

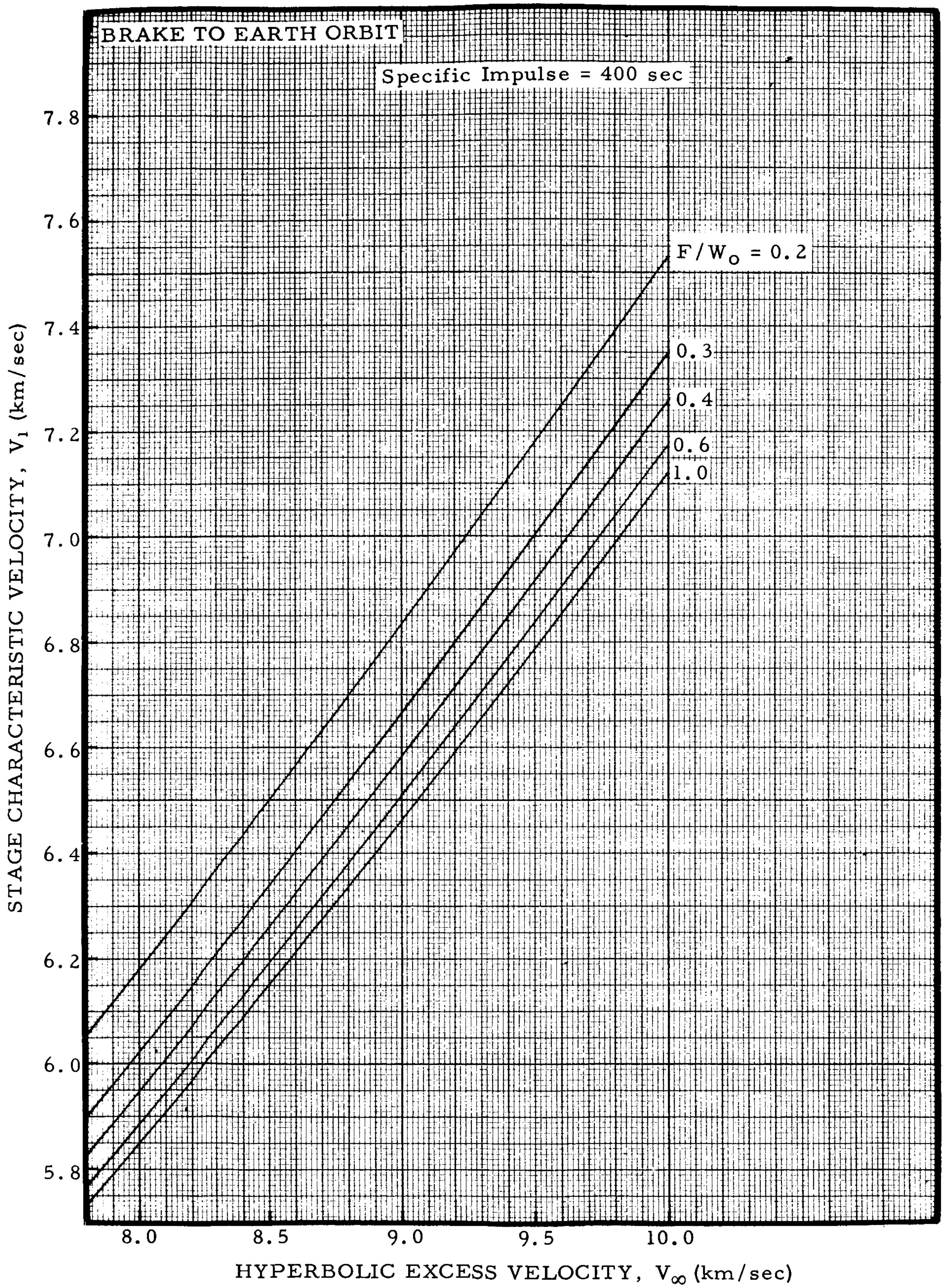

FIGURE 5c. CHARACTERISTIC VELOCITY, V_1 (km/sec), VERSUS HYPERBOLIC EXCESS VELOCITY, V_∞ (km/sec), WITH THRUST-TO-WEIGHT RATIO AS A PARAMETER FOR A CONSTANT SPECIFIC IMPULSE OF 400 SECONDS

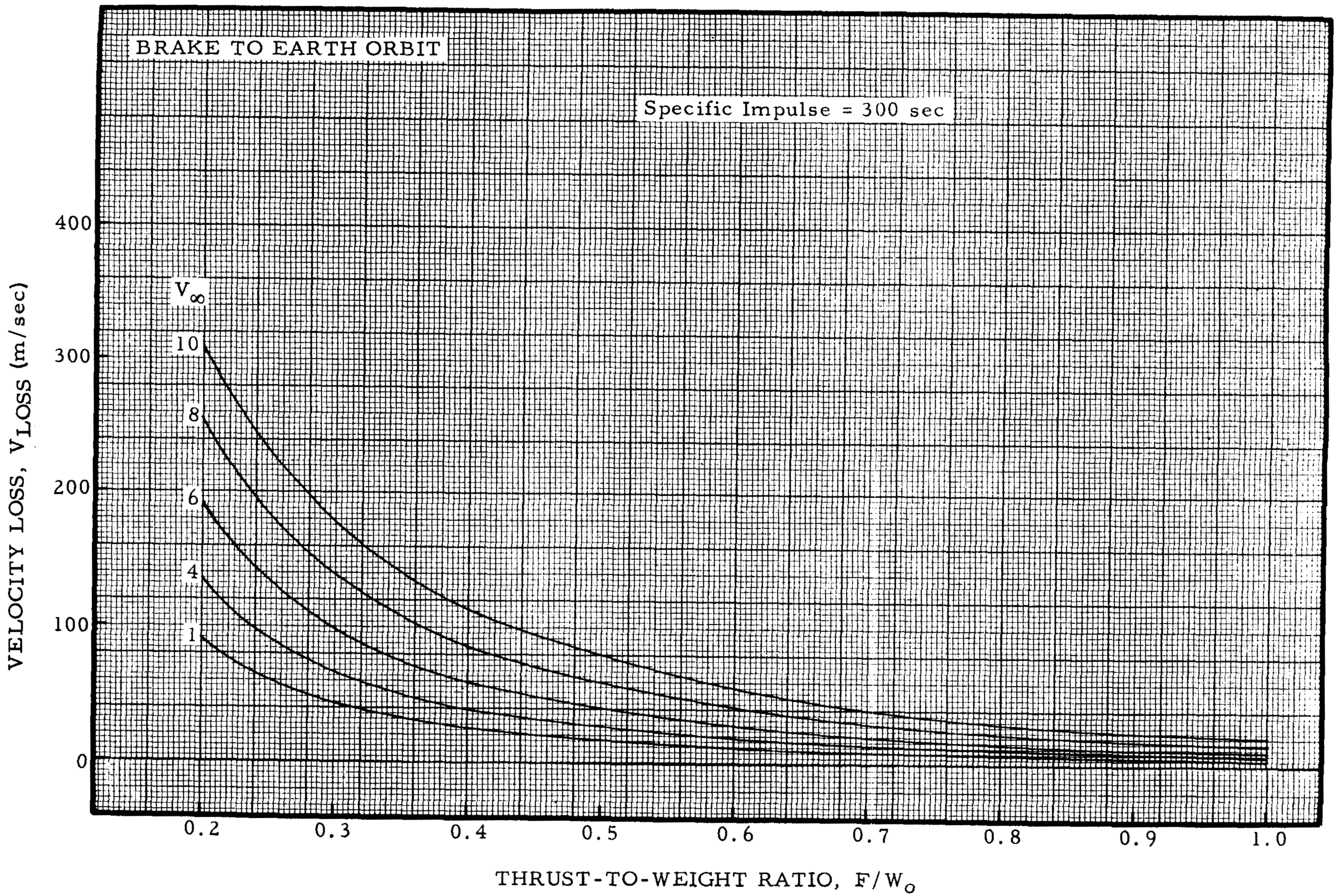

FIGURE 6. VELOCITY LOSS (m/sec) DUE TO GRAVITY VERSUS THRUST-TO-WEIGHT RATIO WITH HYPERBOLIC EXCESS VELOCITY, V_∞ (km/sec), AS A PARAMETER FOR A CONSTANT SPECIFIC IMPULSE OF 300 SECONDS

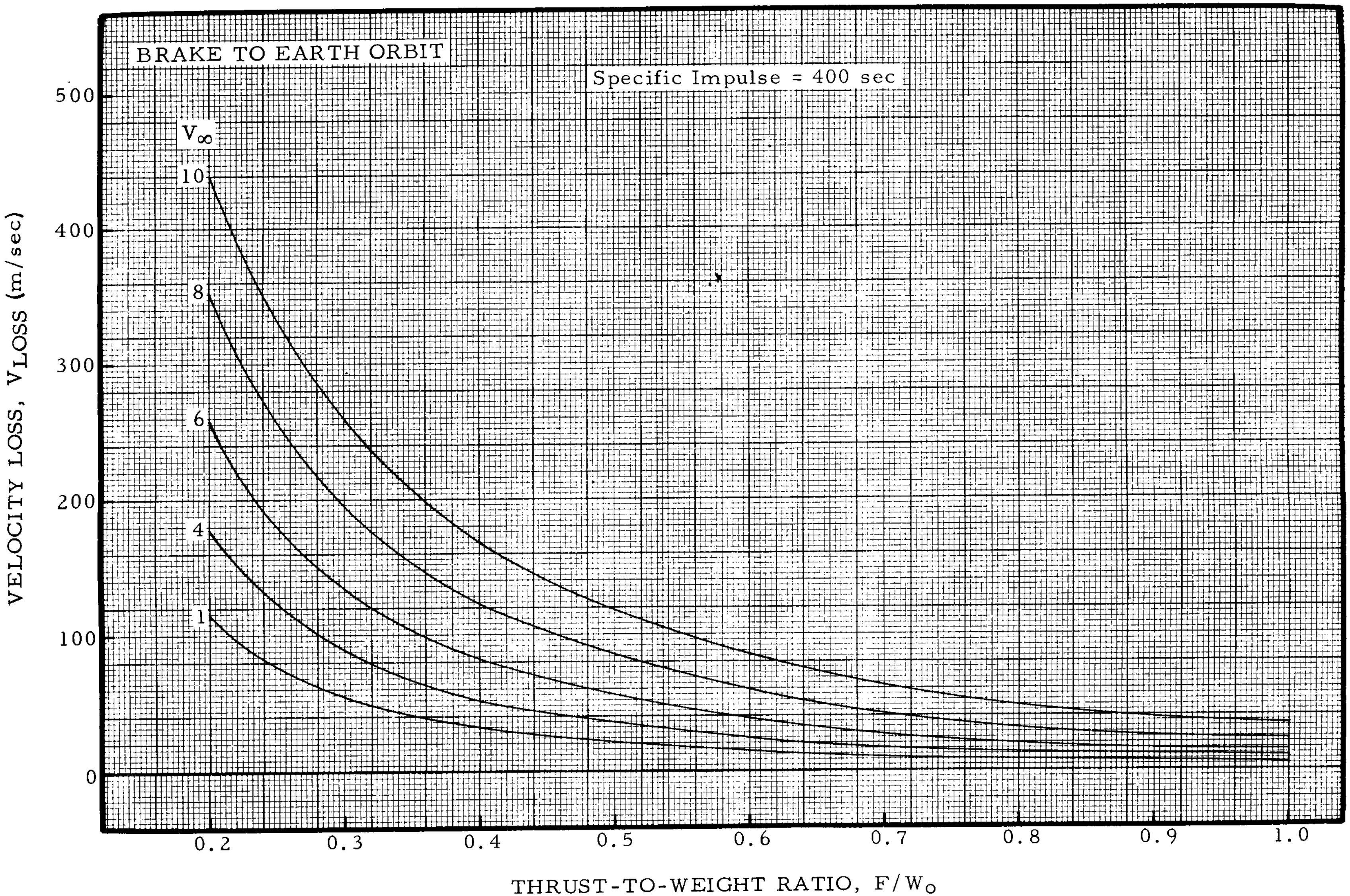

FIGURE 7. VELOCITY LOSS (m/sec) DUE TO GRAVITY VERSUS THRUST-TO-WEIGHT RATIO WITH HYPERBOLIC EXCESS VELOCITY, V_∞ (km/sec), AS A PARAMETER FOR A CONSTANT SPECIFIC IMPULSE OF 400 SECONDS

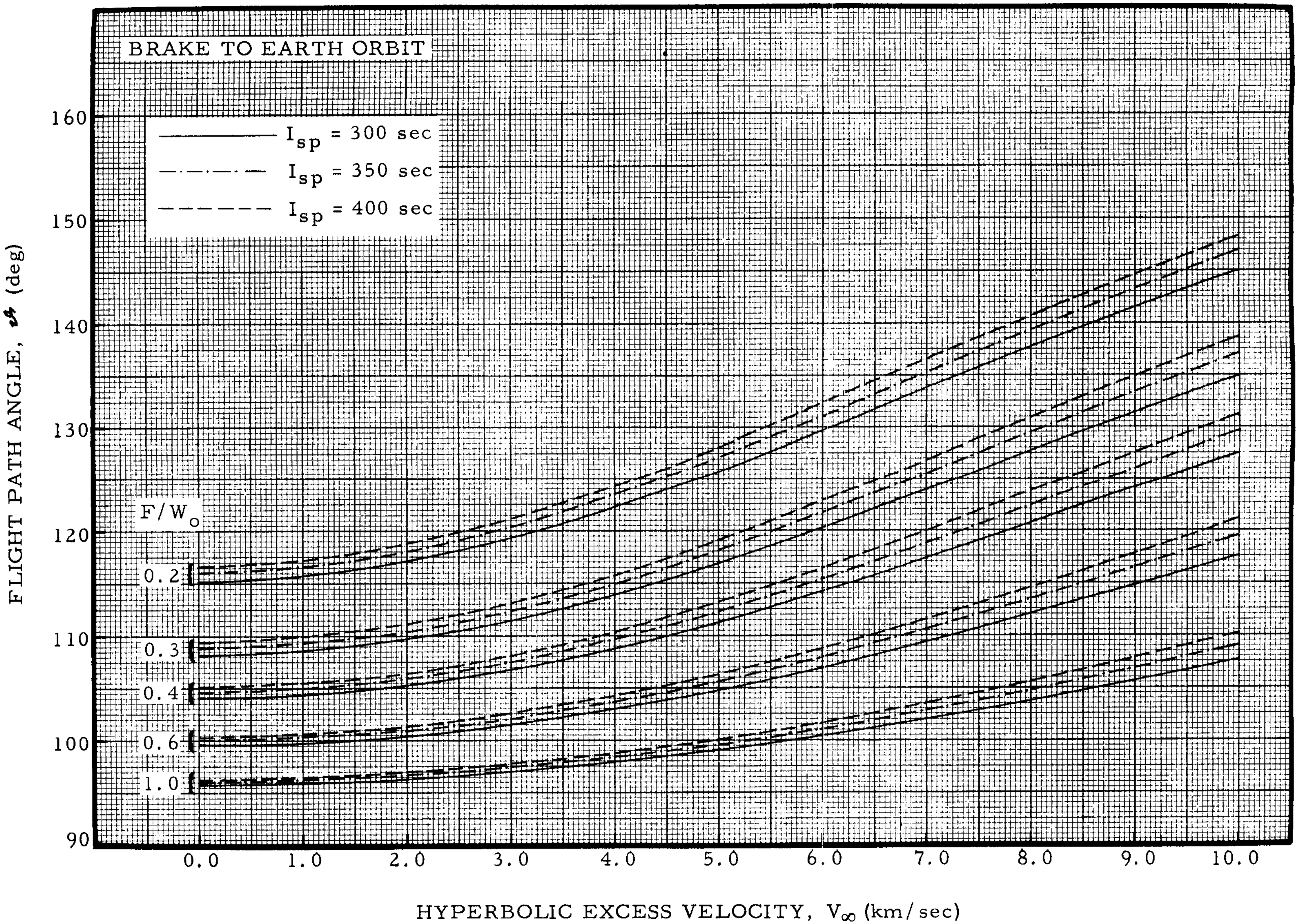

FIGURE 8. FLIGHT PATH ANGLE (deg) VERSUS HYPERBOLIC EXCESS VELOCITY (km/sec) WITH THRUST-TO-WEIGHT RATIO AS A PARAMETER

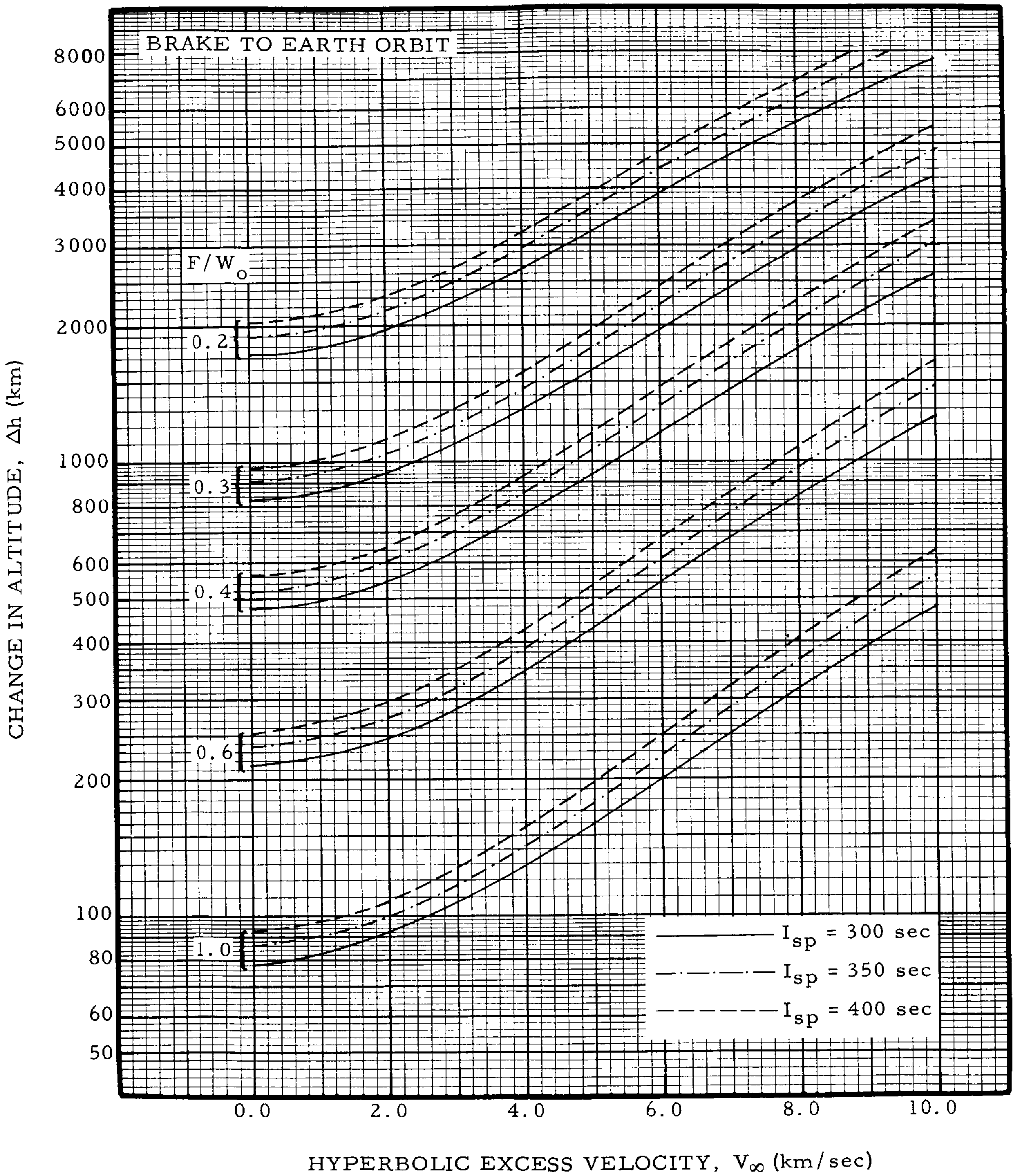

FIGURE 9. CHANGE IN ALTITUDE (km) VERSUS HYPERBOLIC EXCESS VELOCITY (km/sec) WITH THRUST-TO-WEIGHT RATIO AS A PARAMETER

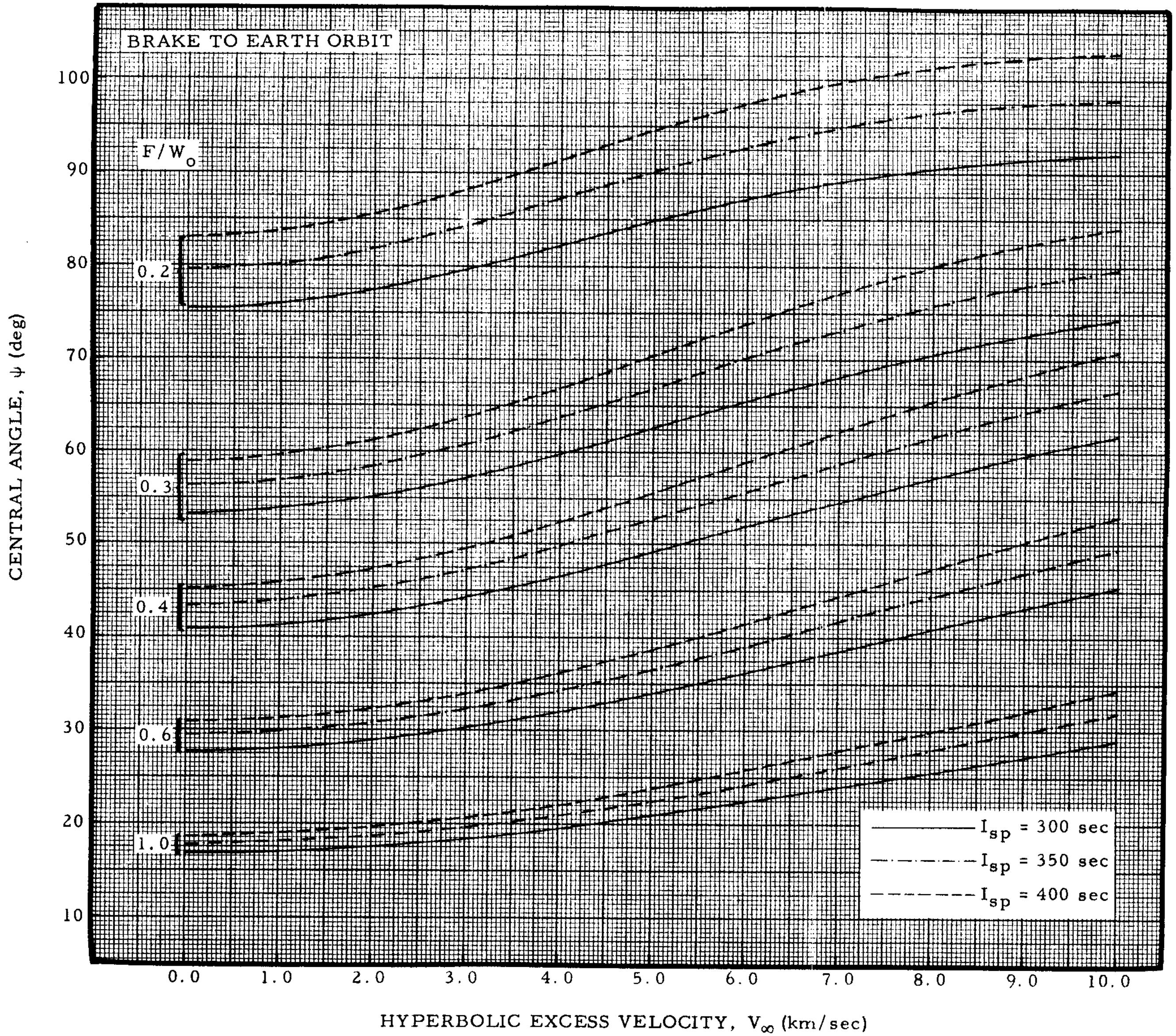

FIGURE 10. CENTRAL ANGLE (deg) VERSUS HYPERBOLIC EXCESS VELOCITY (km/sec) WITH THRUST-TO-WEIGHT RATIO AS A PARAMETER

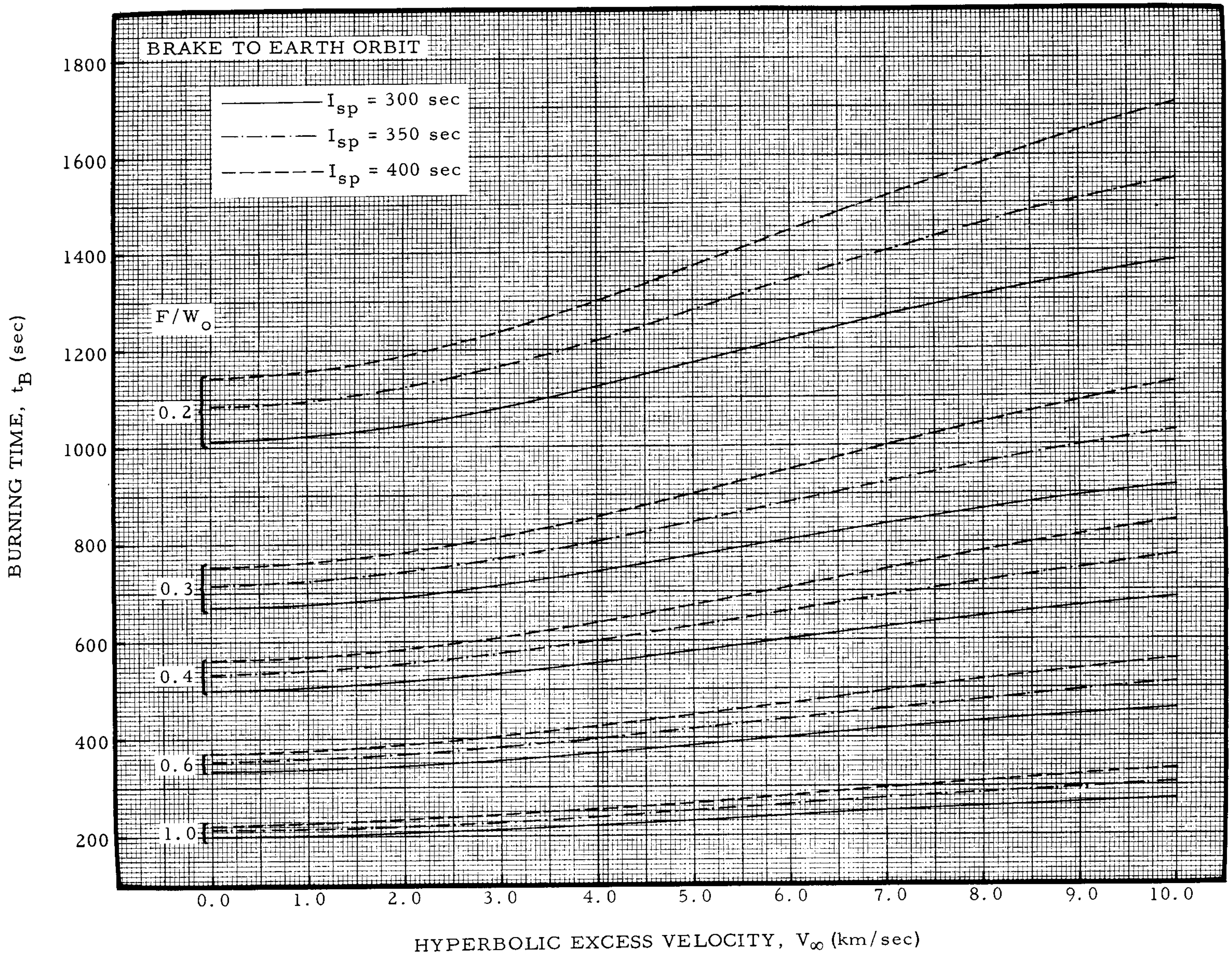

FIGURE 11. BURNING TIME (sec) VERSUS HYPERBOLIC EXCESS VELOCITY (km/sec) WITH THRUST-TO-WEIGHT RATIO AS A PARAMETER

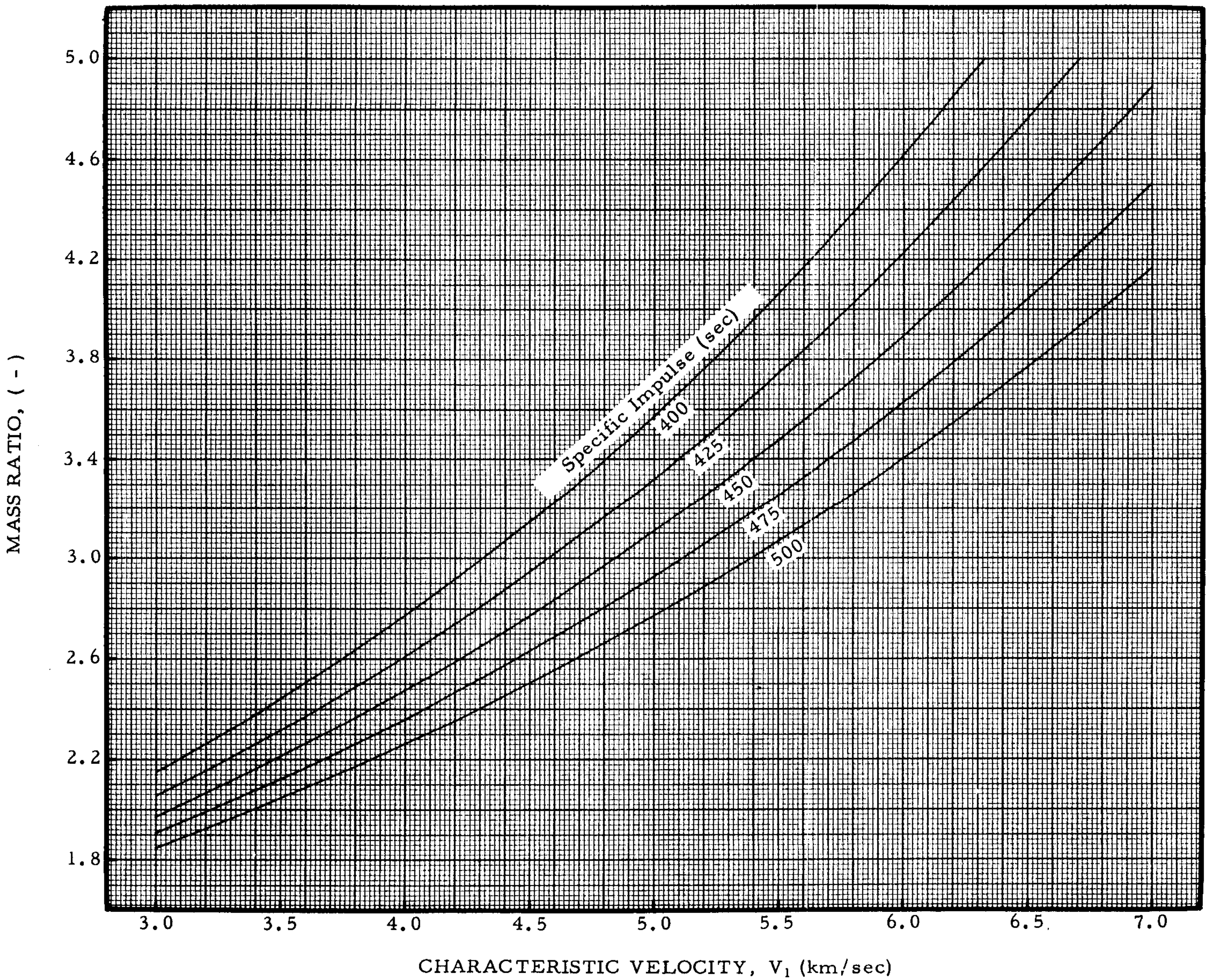

FIGURE 12. MASS RATIO VERSUS CHARACTERISTIC VELOCITY (km/sec) WITH SPECIFIC IMPULSE AS A PARAMETER

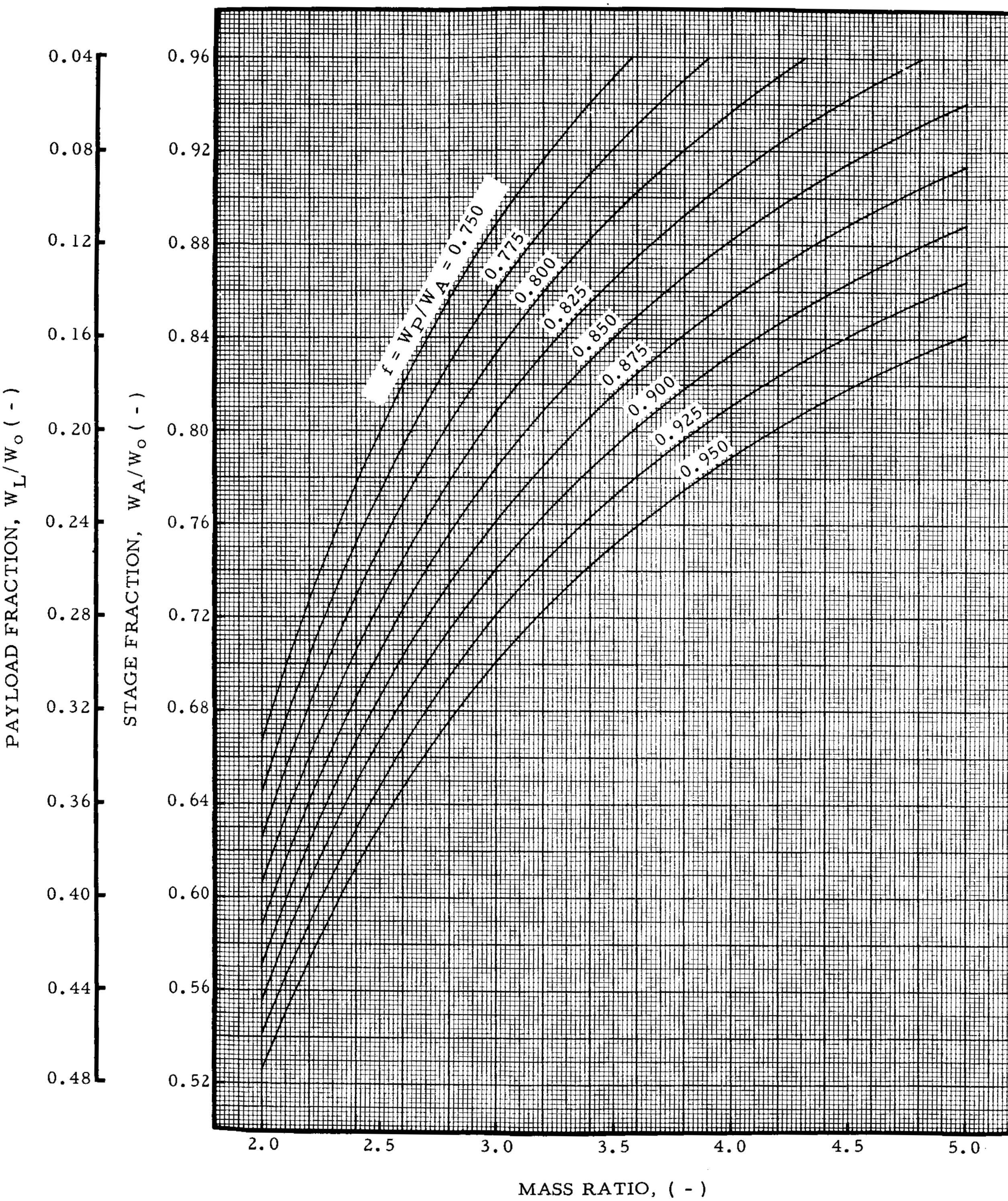

FIGURE 13. PAYLOAD FRACTION AND STAGE FRACTION VERSUS MASS RATIO WITH STAGE MASS FRACTION AS A PARAMETER

BIBLIOGRAPHY

Cavicchi, Richard H. and Miser, James W., Determination of Nuclear-Rocket Power Levels for Unmanned Mars Vehicle Starting from Orbit About Earth. NASA TN D-474, January 1962.

Clarke, Victor C., A Summary of the Characteristics of Ballistic Interplanetary Trajectories, 1962-1977. Jet Propulsion Laboratory, California Institute of Technology, Pasadena, California, Technical Report No. 32-209, NASA Contract No. 7-100, January 15, 1962.

Dobson, Wilbur F., Mackay, John S. and Huff, Vearl N., Starting Conditions for Nonoscillatory Low-Thrust Planet-Escape Trajectories. NASA TN D-1410, August 1962.

Ehricke, Krafft A., Space Flight Principles of Guided Missile Design. (Edited by Grayson Merrill), Princeton, New Jersey, D. Van Nostrand Company, Inc., 1960.

Friedlander, Alan L., A Study of Guidance Sensitivity for Various Low-Thrust Transfers from Earth to Mars. NASA TN S-1183, February 1962.

Friedlander, Alan L. and Harry, David P. III, A Study of Statistical Data-Adjustment and Logic Techniques as Applied to the Interplanetary Midcourse Guidance Problem. NASA TR R-113, 1961.

Knip, Gerald, Jr. and Zola, Charles L., Three-Dimensional Sphere-of-Influence Analysis of Interplanetary Trajectories to Mars. NASA TN D-1199, May 1962.

Knip, Gerald, Jr. and Zola, Charles L., Three-Dimensional Trajectory Analysis for Round-Trip Missions to Mars. NASA TN D-1316, October 1962.

Melbourne, W. G., Richardson, D. E. and Sauer, C. G., Interplanetary Trajectory Optimization with Power-Limited Propulsion Systems. Jet Propulsion Laboratory, California Institute of Technology, Pasadena, California, Technical Report No. 32-173, NASA Contract No. NAS 7-100, February 26, 1962.

Ross, S., et. al., A Study of Interplanetary Transportation Systems. Lockheed Missiles and Space Division, Final Report No. 3-17-62-1, Contract NAS 8-2469, June 2, 1962.

BIBLIOGRAPHY (Concluded)

Soviet Press (February 12 - March 3, 1961), Destination--Venus (Astronautics Information Translation No. 20) Compiled and Translated by Joseph L. Zygielbaum under NASA Contract NASw-6. Jet Propulsion Laboratory, California Institute of Technology, Pasadena, California, April 1, 1961.

Stafford, Walter H., Harlin, Sam H. and Catalfamo, Carmen R., Performance Analysis of High-Energy Chemical Stages for Interplanetary Missions. NASA TN D-1829, January 1964.

Stafford, Walter H. and Harlin, Sam H., Parametric Performance Analysis for Interplanetary Missions Utilizing First-Generation Nuclear Stages, Part I: Departure from Earth Orbit. MSFC Report MTP-P&VE-F-63-14, August 26, 1963.

Stafford, Walter H. and Harlin, Sam H., Parametric Performance Analysis for Interplanetary Missions Utilizing First-Generation Nuclear Stages, Part II: Brake to Venus Orbit. MSFC Report MTP-P&VE-F-63-15, September 1, 1963.

Stafford, Walter H. and Catalfamo, Carmen R., Parametric Performance Analysis for Interplanetary Missions Utilizing First-Generation Nuclear Stages, Part III: Departure from Mars Orbit. MSFC Report MTP-P&VE-F-63-16, September 30, 1963.

Stafford, Walter H. and Harlin, Sam H., Parametric Performance Analysis for Interplanetary Missions Utilizing First-Generation Nuclear Stages, Part IV: Departure from Venus Orbit. MSFC Report MTP-P&VE-A-63-17, October 4, 1963.

Stafford, Walter H. and Catalfamo, Carmen R., Parametric Performance Analysis for Interplanetary Missions Utilizing First-Generation Nuclear Stages, Part V: Brake to Mars Orbit. MSFC Report MTP-P&VE-A-63-18, October 25, 1963.

Zola, Charles L. and Knip, Gerald, Jr., Three-Dimensional Trajectory Analysis for Round-Trip Missions to Venus. NASA TN D-1319, August 1962.